Received: 9 January 2023 | Accepted: 7 June 2023

DOI: 10.1002/acs.3647

RESEARCH ARTICLE

WILEY

Adaptive decentralized prescribed performance control for a class of large-scale stochastic nonlinear systems subject to input saturation and full state constraints

Na Li | **Yang Du** | **Dong-Mei Wang** | **Shan-Liang Zhu** | **Yu-Qun Han**

School of Mathematics and Physics, Qingdao University of Science and Technology, Qingdao, China

Correspondence
Yu-Qun Han, School of Mathematics and Physics, Qingdao University of Science and Technology, Qingdao 266061, China.
Email: yuqunhan@163.com

Funding information
Shandong Provincial Natural Science Foundation, China, Grant/Award Number: ZR2020QF055

Summary

This paper focuses on an adaptive decentralized prescribed performance control problem for a class of large-scale stochastic nonlinear systems with asymmetric input saturation and full state constraints. Firstly, the obstacle of input saturation is overcome by introducing the Gaussian error functions. Secondly, the transient performance of the system output is realized by introducing the asymmetric error transfer functions. Thirdly, the full state constraints are considered in the backstepping control process, and the boundary of state constraints is ensured by constructing barrier Lyapunov functions. Then, the multidimensional Taylor network is employed to approximate the unknown nonlinearity, and an adaptive decentralized controller is designed. Finally, it is shown that the proposed control strategy can ensure that the closed-loop system is semi-global ultimately uniformly bounded in probability, and the tracking error of the system can be kept within an adjustable neighborhood of the origin. Two simulation examples are provided to illustrate the feasibility of the proposed control strategy.

KEYWORDS

decentralized control, full state constraints, input saturation, large-scale stochastic nonlinear systems, prescribed performance control

1 | INTRODUCTION

In the past decades, the research on tracking control of large-scale nonlinear systems has received extensive attention. Due to its strong pertinence and system adaptability, decentralized control has been widely used to study the control problems of large-scale nonlinear systems.[1-3] In recent years, stochastic disturbances inevitably appear in the systems and it is the source of system instability. As a result, the study on large-scale stochastic nonlinear systems gained considerable interest and produced a lot of meaningful results by employing decentralized control methods.[4-6] At the same time, many approximation-based adaptive control methods, such as adaptive neural networks (NNs) control,[7-9] adaptive fuzzy logic systems (FLSs) control[10-12] and adaptive multidimensional Taylor network (MTN) control,[13] have been applied to large-scale stochastic nonlinear systems. As a new type of network, the MTN has been used to solve the control problems of nonlinear systems,[14,15] stochastic nonlinear systems,[16,17] multi-input multi-output (MIMO) nonlinear systems,[18] and large-scale nonlinear systems.[19,20] Nevertheless, although the research of large-scale stochastic

nonlinear systems based on MTN approximation has advanced significantly,[13,20] the question of how to achieve the control objects of the system while taking into account asymmetric input saturation and full state constraints is still a challenging topic.

On the one hand, the input saturation phenomenon exists widely in practical engineering, which will cause system instability. To deal with the negative effect caused by input saturation, two kinds of control methods have been proposed: the saturation compensation method[21] and the saturation approximation method.[22] Compared with the former, the latter employs a smooth function to directly approximate the saturation nonlinearity in the system, which requires little computational effort. Recently, a growing attention has been paid to the combination of the approximation method and adaptive control, and many interesting results have been achieved.[23-25] On the other hand, the phenomenon of state constraints, which may causes the control system performance degradation or even instability, is widely existed in practical systems. Up to now, the construction of barrier Lyapunov functions (BLFs) has become one of the most common methods to deal with state constraints. This method has been successfully applied to general nonlinear systems,[26-28] stochastic nonlinear systems,[29-31] MIMO nonlinear systems,[32,33] and large-scale systems.[34,35] Unfortunately, due to the complexity of the systems structure and the influence of stochastic disturbances, it is very rare to study large-scale stochastic nonlinear systems with input saturation or full state constraints. It is worth noting that the above achievements mainly focus on the steady-state performance of the systems, while ignoring the transient performance of the systems. In practical application, the control system should not only meet certain steady-state performance requirements, but also meet certain stability and response speed requirements in its response process, that is, to achieve the transient performance of the controlled system.

To address the aforementioned issues, the prescribed performance control (PPC) approach has bee proposed. The core idea of PPT method is to limit the tracking error to the given performance envelope function, and characterize the transient and steady-state of the controlled system through the convergence characteristics of the performance envelope function. With the help of FLSs or NNs approximation, integrating PPC approach into backstepping, a series of extensions have been obtained for different systems, such as nonlinear systems with actuator faults,[36,37] nonlinear systems with dynamic uncertainty,[38] nonlinear systems with input constraints,[39,40] MIMO nonlinear systems,[41] and large-scale nonlinear systems with input constraints.[42-44] However, as far as we know, no literature has been devoted to the adaptive MTN-based tracking control for large-scale stochastic nonlinear systems with input saturation and full-state constraints under prescribed performance, which is an interesting topic worth discussing.

Based on the above discussion, an adaptive decentralized PPC strategy based on the MTN is proposed for a class of large-scale stochastic nonlinear systems with input saturation and full state constraints. Firstly, the asymmetric input saturation model is linearized by introducing an auxiliary function. Secondly, BLFs are constructed to deal with state constraints. Finally, based on MTN approximation method, a simple and effective adaptive decentralized PPC strategy is proposed. Compared with the existing results, the main innovations of this paper are as follows:

(i) This study investigates the tracking control problems for a class of large-scale stochastic nonlinear systems, which takes both the input saturation and the full-state constraints into account. A new MTN-based decentralized PPC strategy is proposed via backstepping technique, whch can successfully obtain the ideal control performance under prescribed performance. Although many meaningful MTN-based results have been proposed for large-scale nonlinear systems,[13,20,42,43,45] the issues of PPC, input saturation and full state constraints were not considered simultaneously. Specifically, compared with the existing results without considering the effect of the input and state constraints in References 13 and 20 or the external interference in References 42, 43, and 45, this paper obtained results consider more actual situations.

(ii) In order to overcome the difficulties in controller design brought by the input saturation, a Gaussian error function is employed, which can transform the nonlinear input saturation into a linear function with a bounded error. Besides, introducing a novel coordinate transformation, and combining the prescribed performance function and barrier Lyapunov function can ensure the tracking error converges to the predetermined allowable range, and ensure all states are not violating the given constraint bounds.

(iii) Although input saturation and full state constraints are taken into account in stochastic nonlinear systems,[30,46-48] this paper studies the PPC of large-scale stochastic nonlinear systems, which is more significance in practice. In addition, compared with the existing PPC strategies for large-scale nonlinear systems,[43,44] the influence of stochastic disturbances is considered in this paper, and the input and state constraints are imposed on the controlled system. Therefore, our obtained results consider more actual situations.

2 | PRELIMINARY PREPARATION OF PROBLEMS

2.1 | Stability theory preparation

Consider the following stochastic nonlinear system

$$d\boldsymbol{x} = f(\boldsymbol{x})\,dt + g(\boldsymbol{x})\,d\omega, \quad \forall \boldsymbol{x} \in R^n, \tag{1}$$

where $\boldsymbol{x} \in R^n$ is the state vector, $f : R^n \times R^+ \to R^n, g : R^n \times R^+ \to R^{n\times r}$ are locally Lipschitz functions and satisfy $f(\mathbf{0}) = \mathbf{0}$ and $g(\mathbf{0}) = \mathbf{0}$. ω is an r-dimensional independent standard Wiener process.

Definition 1 ((Reference 49)). For any positive definite function $\Gamma(\boldsymbol{x}, t) \in C^2$ associated with the stochastic nonlinear system (1), define the differential operator as follows

$$L\Gamma = \frac{\partial \Gamma}{\partial \boldsymbol{x}} f + \frac{1}{2} Tr\left\{ g^{\mathrm{T}} \frac{\partial^2 \Gamma}{\partial \boldsymbol{x}^2} g \right\}, \tag{2}$$

where the $Tr\{\cdot\}$ represents the trace of $\cdot$.

Definition 2 ((Reference 12)). For the system (1), if for any initial state $\boldsymbol{x}_0 = \boldsymbol{x}(t_0) \in \Sigma$ with Σ is a compact set, there exist two constants $\varepsilon > 0$ and $T(\varepsilon, \boldsymbol{x}_0)$ such that $E(\|\boldsymbol{x}(t)\|^q) < \varepsilon$ for $t > t_0 + T$, then the trajectory $\{\boldsymbol{x}(t), t \geq 0\}$ of the system (1) is said to be semi-global uniformly ultimately bounded (SGUUB) in qth moment.

Lemma 1 ((Reference 49)). *Consider the system (1), if there is a Lyapunov function $\Gamma(\boldsymbol{x}) \in C^2$ satisfies the inequalities*

$$\ell_1(|\boldsymbol{x}|) \leq \Gamma(\boldsymbol{x}) \leq \ell_2(|\boldsymbol{x}|), \tag{3}$$

$$L\Gamma(\boldsymbol{x}) \leq -\lambda\Gamma(\boldsymbol{x}) + \tau, \tag{4}$$

where $\ell_1(\cdot)$, $\ell_2(\cdot)$ are class κ_∞ function, $\lambda > 0$, $\tau > 0$ are positive constants. Then, the system (1) almost certainly has a unique solution, and the trajectory of the solution is almost bounded.

2.2 | Problem formulation

In this paper, the following large-scale stochastic nonlinear system with N subsystems is considered

$$\begin{cases} dx_{i,j} = \left[x_{i,j+1} + \Phi_{i,j}(\bar{\boldsymbol{x}}_{i,j}) + \mathrm{H}_{i,j}(\boldsymbol{y})\right] dt + \Psi_{i,j}^{\mathrm{T}}(\boldsymbol{y}) d\omega_i, & j = 1, \ldots, n_i - 1 \\ dx_{i,n_i} = \left[u_i(v_i) + \Phi_{i,n_i}(\bar{\boldsymbol{x}}_{i,n_i}) + \mathrm{H}_{i,j}(\boldsymbol{y})\right] dt + \Psi_{i,n_i}^{\mathrm{T}}(\boldsymbol{y}) d\omega_i & \\ y_i = x_{i,1} & \end{cases}, \tag{5}$$

where $i = 1, 2, \ldots, N$. $x_{i,1}, x_{i,2}, \ldots, x_{i,j}$ represent the measurable states of the ith subsystem, which are constrained in the compact sets, that is, $|x_{i,j}| < B_{i,j}$ with $B_{i,j}$ are known constraint constants, $\bar{\boldsymbol{x}}_{i,j} = \left[x_{i,1}, x_{i,2}, \ldots, x_{i,j}\right]^{\mathrm{T}} \in R^j$. y_i represents the output of the ith subsystem with $\boldsymbol{y} = [y_1, y_2, \ldots, y_N]^{\mathrm{T}} \in R^N$. ω_i is an r_i-dimensional independent standard Wiener process. $\Phi_{i,j}(\cdot) : R^j \to R$ denotes the unknown nonlinear continuous function and satisfies $\Phi_{i,j}(\mathbf{0}) = \mathbf{0}$. Moreover, $\mathrm{H}_{i,j}(\cdot) : R^N \to R$ and $\Psi_{i,j}(\cdot) : R^N \to R$ are unknown smooth nonlinear functions with $\mathrm{H}_{i,j}(\mathbf{0}) = 0$ and $\Psi_{i,j}(\mathbf{0}) = \mathbf{0}$, which represent the interconnection between subsystems. $u_i(v_i)$ represents the input saturation nonlinearity, which can be expressed as follows

$$u_i(v_i) = Sat[v_i] = \begin{cases} u_{i,\min}, & v_i < u_{i,\min} \\ v_i, & u_{i,\min} \leq v_i \leq u_{i,\max} \\ u_{i,\max}, & v_i > u_{i,\max} \end{cases},$$

where v_i denotes the input signal, $u_{i,\min}$ and $u_{i,\max}$ denote the lower and upper bounds of the actuator u_i.

The purpose of this paper is to develop an adaptive control strategy for system (5), such that

(1) All signals of the closed-loop system are SGUUB in probability.
(2) All states $x_{i,j}, i = 1, \ldots, N; j = 1, \ldots, n_i$ are not violating the given constraint bounds.
(3) The desired reference signal $y_{r,i}, i = 1, 2, \ldots, N$ is well tracked by the output y_i of ith subsystem. Furthermore, the tracking error $e_i = y_i - y_{r,i}$ of the closed-loop system (5) converges to the predetermined allowable range.

The saturation model clearly shows that there are two sharp angles between the control input and the control output, implying that it cannot be employed directly in the backstepping process. Therefore, an approximation-based approach is used to eliminate the influence of input saturation, similar to work,[46] a input saturation nonlinear smooth model is introduced, which is mathematically described as follows

$$u_i(v_i) = \bar{u}_i erf\left(\left(\sqrt{\pi}/2\bar{u}_i\right)v_i\right), \tag{6}$$

where $\bar{u}_i = \frac{u_{i,\max}+u_{i,\min}}{2} + \frac{u_{i,\max}-u_{i,\min}}{2} sign(v_i)$ with sign $(\cdot)$ is a standard symbolic function, erf $(\cdot)$ is a Gaussian error function expressed as $\text{erf}(x) = \frac{2}{\pi}\int_0^x e^{-t^2}dt$.

Remark 1. Define a new function $\Theta_i(v_i)$ as $\Theta_i(v_i) = u_i - \eta_i v_i$, where $\eta_i > 0$ is a positive constant. Then, the u_i can be rewritten as follows

$$u_i = \eta_i v_i + \Theta_i(v_i). \tag{7}$$

Throughout this paper, the following preliminaries and relevant preparations need to be made on the system (5).

Assumption 1 ((References 13 and 32)). The desired reference signal $y_{r,i}$ and its ith derivative $y_{r,i}^{(i)}$ are continuous and satisfy $|y_{r,i}| \le \gamma_0 \le B_{i,1}$ and $\left|y_{r,i}^{(i)}\right| \le \varpi_i$, where $\gamma_0 > 0$ and $\varpi_i > 0$ are constants.

Assumption 2 ((Reference 13)). For the unknown smooth functions $\mathrm{H}_{i,j}(\boldsymbol{y})$ and $\Psi_{i,j}(\boldsymbol{y})$, there exist known smooth functions $\mathrm{H}_{i,j,k}(y_k)$ and $\Psi_{i,j,k}(y_k)$, such that

$$\left|\mathrm{H}_{i,j}(\boldsymbol{y})\right|^2 \le \sum_{k=1}^{N} \mathrm{H}_{i,j,k}^2(y_k), \tag{8}$$

$$\left\|\Psi_{i,j}(\boldsymbol{y})\right\|^2 \le \sum_{k=1}^{N} \Psi_{i,j,k}^2(y_k), \tag{9}$$

where $\mathrm{H}_{i,j,k}(\cdot)$ and $\Psi_{i,j,k}(\cdot)$ are the analytic functions with $\mathrm{H}_{i,j,k}(0) = 0$ and $\Psi_{i,j,k}(0) = 0$.

Remark 2. According to Assumption 2, the origin is the equilibrium point of the ith subsystem. Based on mean value theorem, there exist unknown smooth nonlinear functions $\bar{\mathrm{H}}_{i,j,k}(y_k)$ and $\bar{\Psi}_{i,j,k}(y_k)$ such that inequalities $\left|\mathrm{H}_{i,j}(\boldsymbol{y})\right|^2 \le \sum_{k=1}^{N} y_k^2 \bar{\mathrm{H}}_{i,j,k}^2(y_k)$ and $\left\|\Psi_{i,j}(\boldsymbol{y})\right\|^2 \le \sum_{k=1}^{N} y_k^2 \bar{\Psi}_{i,j,k}^2(y_k)$ can be obtained.

Lemma 2 *((Reference 26)). For $\forall \varphi_i \in R$ satisfies $|\varphi_i| < K_{a,i}$ with $K_{a,i}$ is a positive constant, the following inequality is holds*

$$\log \frac{K_{a,i}^{2p}}{K_{a,i}^{2p} - \varphi_i^{2p}} < \frac{\varphi_i^{2p}}{K_{a,i}^{2p} - \varphi_i^{2p}}, \tag{10}$$

where $\log(\cdot)$ *is a logarithm of* $(\cdot)$ *and p is a positive constant.*

For the processing of input saturation, the following assumption is required.

Assumption 3 ((Reference 30)). For formula (7) defined previously, we assume that there are constant $\overline{\Theta}$ and positive constants $\sigma_{i,1}, \sigma_{i,2}$, so that $\Theta_i(v_i) \le \bar{\Theta}$ and $\eta_i \in [\sigma_{i,1}, \sigma_{i,2}]$ are satisfied.

2.3 | Multidimensional Taylor network

In this article, the unknown nonlinearity in the controlled system is approximated by MTN. Considering that the concept of MTN-based control has been mentioned in References 13, 20, and 49, only the following useful lemma is presented.

Lemma 3 ((Reference 43)). *Supposing there is a continuous nonlinear function $M(\boldsymbol{\varphi})$ defined on a compact set $\Lambda \subset R^n$, for $\forall \varepsilon > 0$, $M(\boldsymbol{\varphi})$ can be approximated by $\boldsymbol{\vartheta}^{\mathrm{T}} P_{m_n}$ in the following way*

$$M(\boldsymbol{\varphi}) = \boldsymbol{\vartheta}^{\mathrm{T}} P_{m_n}(\boldsymbol{\varphi}) + \delta(\boldsymbol{\varphi}), \quad |\delta(\boldsymbol{\varphi})| \leq \varepsilon, \tag{11}$$

where $\boldsymbol{\varphi} = [\varphi_1, \varphi_2, \ldots, \varphi_n]^{\mathrm{T}} \in \Lambda \subset R^n$ and $\boldsymbol{\vartheta} = [\vartheta_1, \vartheta_2, \ldots, \vartheta_\kappa]^{\mathrm{T}} \in R^\kappa$ represent the input vector and weight vector of MTN, respectively. $P_{m_n}(\boldsymbol{\varphi}) = [\varphi_1, \ldots, \varphi_n, \varphi_1^2, \varphi_1\varphi_2, \ldots, \varphi_1\varphi_n, \varphi_2^2, \ldots \varphi_n^2, \ldots, \varphi_1^m, \ldots, \varphi_n^m]^{\mathrm{T}} \in R^\kappa$ denotes middle layer, which is the polynomial combination of the input layer with n and κ are the input and dimension. Moreover, $\delta(\boldsymbol{\varphi})$ is the approximation error.

3 | CONTROLLER DESIGN AND STABILITY ANALYSIS

In this section, an adaptive decentralized PPC tracking design scheme is proposed based on the backstepping design framework. Before the control design, the following theories about the PPC are given.

Firstly, define the coordinate changes as follows

$$\begin{cases} e_i = x_{i,1} - y_{r,i} \\ \varphi_{i,j} = x_{i,j} - \alpha_{i,j-1}, \qquad j = 2, 3, \ldots, n_i \end{cases}, \tag{12}$$

where $i = 1, \ldots, N$, $\alpha_{i,j-1}$ are the virtual control signals, which will be designed later.

In order to limit the error e_i to the bounds $-\delta_{i,1} w_{i,1}(t) \leq e_i(t) \leq \delta_{i,2} w_{i,1}(t)$ for $\forall t \geq 0$, with the help of Reference 44, the following prescribed performance function is introduced

$$w_{i,1}(t) = \left(w_{i,0} - w_{i,\infty}\right) e^{-l_i t} + w_{i,\infty},$$

where $\delta_{i,1}$ and $\delta_{i,2}$ are positive design parameters, $w_{i,0} = w_{i,1}(0)$, $w_{i,0}, w_{i,\infty}$ and l_i are positive constants with $w_{i,0} > w_{i,\infty} > 0$.

Secondly, for $\forall t \geq 0$, define the error conversion as $e_i(t) = w_{i,1}(t)\,\mathrm{B}_{i,1}\left(\zeta_{i,1}(t)\right)$ with $\mathrm{B}_{i,1}\left(\zeta_{i,1}\right) = \frac{\delta_{i,2} e^{\zeta_{i,1}} - \delta_{i,1} e^{-\zeta_{i,1}}}{e^{\zeta_{i,1}} + e^{-\zeta_{i,1}}}$ and $\zeta_{i,1}(t)$ is the transformed error. Further, it can be obtained that $\zeta_{i,1}(t) = \frac{1}{2} \ln \frac{\mathrm{B}_{i,1} + \delta_{i,1}}{\delta_{i,2} - \mathrm{B}_{i,1}}$, and the derivative of $\zeta_{i,1}$ can be calculated as follows

$$d\zeta_{i,1} = w_{i,1,e} \left(x_{i,2} + \Phi_{i,1} + \mathrm{H}_{i,1} - \dot{y}_{r,i} - \frac{\dot{w}_{i,1} e_i}{w_{i,1}} \right) dt + w_{i,1,e} \Psi_{i,1} d\omega,$$

where $w_{i,1,e} = \frac{1}{2w_{i,1}} \left[\left(\frac{1}{\mathrm{B}_{i,1} + \delta_{i,1}} \right) + \left(\frac{1}{\delta_{i,2} - \mathrm{B}_{i,1}} \right) \right]$.

Finally, define $\varphi_{i,1} = -\frac{1}{2} \ln \frac{\delta_{i,1}}{\delta_{i,2}} + \zeta_{i,1}(t)$, and introduce the following coordinate transformations before controlling the design

$$\begin{cases} \varphi_{i,1} = -\frac{1}{2} \ln \frac{\delta_{i,1}}{\delta_{i,2}} + \zeta_{i,1} \\ \varphi_{i,j} = x_{i,j} - \alpha_{i,j-1}, \qquad j = 2, 3, \ldots, n_i \end{cases}. \tag{13}$$

3.1 | Design of control strategy

Step i, 1: Constructing the Lyapunov function as follows

$$\Gamma_{i,1} = \frac{1}{4}\log\frac{K_{a,i,1}^4}{K_{a,i,1}^4 - \varphi_{i,1}^4} + \frac{1}{2}\tilde{\boldsymbol{\vartheta}}_{i,1}^{\mathrm{T}}\tilde{\boldsymbol{\vartheta}}_{i,1}, \tag{14}$$

where $K_{a,i,1} = B_{i,1} - \gamma_0$, and $\tilde{\boldsymbol{\vartheta}}_{i,1} = \boldsymbol{\vartheta}_{i,1} - \hat{\boldsymbol{\vartheta}}_{i,1}$ represents the parameter error vector and $\hat{\boldsymbol{\vartheta}}_{i,1}$ is the estimation of $\boldsymbol{\vartheta}_{i,1}$.

According to Definition 1, calculating the derivative of $\Gamma_{i,1}$ with respect to time t as follows

$$L\Gamma_{i,1} = \frac{\varphi_{i,1}^3 w_{i,1,e}}{K_{a,i,1}^4 - \varphi_{i,1}^4}\left(\varphi_{i,2} + \alpha_{i,1} + \Phi_{i,1} + \mathrm{H}_{i,1} - \dot{y}_{r,i} - \frac{e_i\dot{w}_{i,1}}{w_{i,1}}\right) + \frac{\varphi_{i,1}^2\left(3K_{a,i,1}^4 + \varphi_{i,1}^4\right)}{2\left(K_{a,i,1}^4 - \varphi_{i,1}^4\right)^2}\left\|w_{i,1,e}\Psi_{i,1}\right\|^2 - \tilde{\boldsymbol{\vartheta}}_{i,1}^{\mathrm{T}}\dot{\hat{\boldsymbol{\vartheta}}}_{i,1}. \tag{15}$$

Based on Assumption 2 and Remark 2, the following inequalities can be obtained with the help of Young's Inequality

$$\frac{\varphi_{i,1}^3 w_{i,1,e}}{K_{a,i,1}^4 - \varphi_{i,1}^4}\varphi_{i,2} \le \frac{1}{4h_{i,1}^4}\varphi_{i,2}^4 + \frac{3h_{i,1}^{\frac{4}{3}}}{4}\frac{\varphi_{i,1}^4 w_{i,1,e}^{\frac{4}{3}}}{\left(K_{a,i,1}^4 - \varphi_{i,1}^4\right)^{\frac{4}{3}}}, \tag{16}$$

$$\frac{\varphi_{i,1}^3 w_{i,1,e}\mathrm{H}_{i,1}}{K_{a,i,1}^4 - \varphi_{i,1}^4} \le \frac{3\varphi_{i,1}^4 w_{i,1,e}^{\frac{4}{3}}}{4\left(K_{a,i,1}^4 - \varphi_{i,1}^4\right)^{\frac{4}{3}}} + \frac{N}{4}\sum_{k=1}^{N} y_k^4\bar{\mathrm{H}}_{i,1,k}^4, \tag{17}$$

$$\frac{\varphi_{i,1}^2\left(3K_{a,i,1}^4 + \varphi_{i,1}^4\right)\left\|w_{i,1,e}\Psi_{i,1}\right\|^2}{2\left(K_{a,i,1}^4 - \varphi_{i,1}^4\right)^2} \le \frac{\varphi_{i,1}^4\left(3K_{a,i,1}^4 + \varphi_{i,1}^4\right)^2}{4\left(K_{a,i,1}^4 - \varphi_{i,1}^4\right)^4} + \frac{N}{4}\sum_{k=1}^{N} w_{i,1,e}^2 y_k^4\bar{\Psi}_{i,1,k}^4, \tag{18}$$

where $h_{i,1} > 0$ is a constant.

Then, substituting (16), (17), and (18) into (15), the following inequality can be obtained

$$L\Gamma_{i,1} \le \frac{\varphi_{i,1}^3 w_{i,1,e}}{K_{a,i,1}^4 - \varphi_{i,1}^4}\left(\alpha_{i,1} + M_{i,1}\right) + \frac{N}{4}\sum_{k=1}^{N}\left(w_{i,1,e}^2 y_k^4\overline{\Psi}_{i,1,k}^4 + y_k^4\overline{\mathrm{H}}_{i,1,k}^4\right) + \frac{\varphi_{i,2}^4}{4h_{i,1}^4} - \frac{1}{2}\frac{\varphi_{i,1}^6 w_{i,1,e}^2}{\left(K_{a,i,1}^4 - \varphi_{i,1}^4\right)^2} - G_i - \tilde{\boldsymbol{\vartheta}}_{i,1}^{\mathrm{T}}\dot{\hat{\boldsymbol{\vartheta}}}_{i,1}. \tag{19}$$

where $M_{i,1} = \frac{3\varphi_{i,1}w_{i,1,e}^{\frac{1}{3}}\left(h_{i,1}^{\frac{4}{3}}+1\right)}{4\left(K_{a,i,1}^4-\varphi_{i,1}^4\right)^{\frac{1}{3}}} + \frac{\varphi_{i,1}\left(3K_{a,i,1}^4+\varphi_{i,1}^4\right)^2}{4\left(K_{a,i,1}^4-\varphi_{i,1}^4\right)^3 w_{i,1,e}} + \frac{\varphi_{i,1}^3 w_{i,1,e}}{2\left(K_{a,i,1}^4-\varphi_{i,1}^4\right)} + \Phi_{i,1} - \dot{y}_{r,i} - \frac{e_i\dot{w}_{i,1}}{w_{i,1}} + \chi\left(\varphi_{i,1}^2\right)\varphi_{i,1}$ and $G_i = \frac{\chi\left(\varphi_{i,1}^2\right)\varphi_{i,1}^4 w_{i,1,e}}{K_{a,i,1}^4-\varphi_{i,1}^4}$, $\chi\left(\varphi_{i,1}^2\right)$ is a smooth nonnegative function will be designed later.

Obviously, $M_{i,1}$ is an unknown nonlinear function, which cannot be directly used in the design of the controller. According to Lemma 3, for $\forall\varepsilon_{i,1} > 0$, there must be a $\boldsymbol{\vartheta}_{i,1}^{\mathrm{T}}P_{m_{i,1}}$ with approximation error $\delta_{i,1}$, such that

$$M_{i,1}\left(\boldsymbol{\varphi}_{i,1}\right) = \boldsymbol{\vartheta}_{i,1}^{\mathrm{T}}P_{m_{i,1}}\left(\boldsymbol{\varphi}_{i,1}\right) + \delta_{i,1}\left(\boldsymbol{\varphi}_{i,1}\right), \tag{20}$$

where $\boldsymbol{\varphi}_{i,1} = \left[\varphi_{i,1}\right]^{\mathrm{T}}$ denotes the input vector and approximation error $\delta_{i,1}$ satisfies $\left|\delta_{i,1}\left(\boldsymbol{\varphi}_{i,1}\right)\right| \le \varepsilon_{i,1}$.

Then, based on Young's Inequality, the following inequality is holds

$$\frac{\varphi_{i,1}^3 w_{i,1,e}}{K_{a,i,1}^4 - \varphi_{i,1}^4}M_{i,1} \le \frac{\varphi_{i,1}^3 w_{i,1,e}}{K_{a,i,1}^4 - \varphi_{i,1}^4}\boldsymbol{\vartheta}_{i,1}^{\mathrm{T}}P_{m_{i,1}} + \frac{1}{2}\frac{\varphi_{i,1}^6 w_{i,1,e}^2}{\left(K_{a,i,1}^4 - \varphi_{i,1}^4\right)^2} + \frac{1}{2}\epsilon_{i,1}^2. \tag{21}$$

Substituting (21) into (19), we have

$$L\Gamma_{i,1} \leq \frac{\varphi_{i,1}^3 w_{i,1,e}}{K_{a,i,1}^4 - \varphi_{i,1}^4}\left(\alpha_{i,1} + \vartheta_{i,1}^{\mathrm{T}} P_{m_{i,1}}\right) + \frac{\varphi_{i,2}^4}{4h_{i,1}^4} + \frac{\varepsilon_{i,1}^2}{2} + \frac{N}{4}\sum_{k=1}^{N}\left(w_{i,1,e}^2 y_k^4 \bar{\Psi}_{i,1,k}^4 + y_k^4 \bar{\mathrm{H}}_{i,1,k}^4\right) - \tilde{\vartheta}_{i,1}^{\mathrm{T}}\dot{\hat{\vartheta}}_{i,1} - G_i. \tag{22}$$

According to (22), designed the first virtual control signal $\alpha_{i,1}$ as follows

$$\alpha_{i,1} = -\frac{1}{w_{i,1,e}} b_{i,1}\varphi_{i,1} - \hat{\vartheta}_{i,1}^{\mathrm{T}} P_{m_{i,1}} \tag{23}$$

where $b_{i,1} > 0$ is a design constant.

Then, substituting the virtual control signal (23) into (22), the following inequality can be established

$$L\Gamma_{i,1} \leq \frac{-b_{i,1}\varphi_{i,1}^4}{K_{a,i,1}^4 - \varphi_{i,1}^4} + \tilde{\vartheta}_{i,1}^{\mathrm{T}}\left(\frac{\varphi_{i,1}^3}{K_{a,i,1}^4 - \varphi_{i,1}^4} P_{m_{i,1}} - \dot{\hat{\vartheta}}_{i,1}\right) + \frac{N}{4}\sum_{k=1}^{N}\left(w_{i,1,e}^2 y_k^4 \bar{\Psi}_{i,1,k}^4 + y_k^4 \bar{\mathrm{H}}_{i,1,k}^4\right) + \frac{\varphi_{i,2}^4}{4h_{i,1}^4} + \frac{\varepsilon_{i,1}^2}{2} - G_i. \tag{24}$$

In view of (24), constructed the first adaptive law $\dot{\hat{\vartheta}}_{i,1}$ as follows

$$\dot{\hat{\vartheta}}_{i,1} = -\mu_{i,1}\hat{\vartheta}_{i,1} + \frac{\varphi_{i,1}^3 w_{i,1,e}}{K_{a,i,1}^4 - \varphi_{i,1}^4} P_{m,i,1}, \tag{25}$$

where $\mu_{i,1} > 0$ is a design constant.

Then, substituting (25) into (24), the following inequality is easily established

$$L\Gamma_{i,1} \leq \frac{-b_{i,1}\varphi_{i,1}^4}{K_{a,i,1}^4 - \varphi_{i,1}^4} + \frac{N}{4}\sum_{k=1}^{N}\left(w_{i,1,e}^2 y_k^4 \bar{\Psi}_{i,1,k}^4 + y_k^4 \bar{\mathrm{H}}_{i,1,k}^4\right) + \frac{\varphi_{i,2}^4}{4h_{i,1}^4} + \frac{1}{2}\varepsilon_{i,1}^2 + \mu_{i,1}\tilde{\vartheta}_{i,1}^{\mathrm{T}}\hat{\vartheta}_{i,1} - G_i. \tag{26}$$

Step i, 2: Constructing the following Lyapunov function

$$\Gamma_{i,2} = \Gamma_{i,1} + \frac{1}{4}\log\frac{K_{a,i,2}^4}{K_{a,i,2}^4 - \varphi_{i,2}^4} + \frac{1}{2}\tilde{\vartheta}_{i,2}^{\mathrm{T}}\tilde{\vartheta}_{i,2}, \tag{27}$$

where $K_{a,i,2} = B_{i,2} - \gamma_1$ with γ_1 is a positive constant, $\tilde{\vartheta}_{i,2} = \vartheta_{i,2} - \hat{\vartheta}_{i,2}$ represents the parameter error vector, and $\hat{\vartheta}_{i,2}$ is the estimation of $\vartheta_{i,2}$.

Calculating the derivative of $\Gamma_{i,2}$ with respect to time t as follows

$$L\Gamma_{i,2} = L\Gamma_{i,1} + \frac{\varphi_{i,2}^3}{K_{a,i,2}^4 - \varphi_{i,2}^4}\left(x_{i,3} + \Phi_{i,2} + \mathrm{H}_{i,2} - \nabla\alpha_{i,1}\right) + \frac{\varphi_{i,2}^2}{2\left(K_{a,i,2}^4 - \varphi_{i,2}^4\right)^2}\left(3K_{a,i,2}^4 + \varphi_{i,2}^4\right)\|F_{i,2}\|^2 - \tilde{\vartheta}_{i,2}^{\mathrm{T}}\dot{\hat{\vartheta}}_{i,2}, \tag{28}$$

where $\nabla\alpha_{i,1} = \left(\frac{\partial\alpha_{i,1}}{\partial x_{i,1}}\left(x_{i,2} + \Phi_{i,1} + \mathrm{H}_{i,1}\right) + \frac{\partial\alpha_{i,1}}{\partial\hat{\vartheta}_{i,1}}\dot{\hat{\vartheta}}_{i,1} + \frac{\partial\alpha_{i,1}}{\partial w_{i,1}}\dot{w}_{i,1}\right) + \sum_{j=0}^{1}\frac{\partial\alpha_{i,1}}{\partial y_{r,i}^{(j)}} y_{r,i}^{(j+1)} + \frac{1}{2}\sum_{p,q=1}^{1}\frac{\partial^2\alpha_{i,1}}{\partial x_{i,p}x_{i,q}}\Psi_{i,p}^{\mathrm{T}}\Psi_{i,q}$ and $F_{i,2} = \Psi_{i,2} - \frac{\partial\alpha_{i,1}}{\partial x_{i,1}}\Psi_{i,1}$.

Similar to the step 1, based on Assumption 2 and Remark 2, the following inequality can be obtained with the help of Young's Inequality

$$\begin{aligned} L\Gamma_{i,2} \leq\ & L\Gamma_{i,1} + \frac{\varphi_{i,2}^3}{K_{a,i,2}^4 - \varphi_{i,2}^4}\left(\alpha_{i,2} + M_{i,2}\right) + \frac{N}{4}\sum_{k=1}^{N}\left(y_k^4 \bar{\mathrm{H}}_{i,2,k}^4 + y_k^4 \bar{\Psi}_{i,2,k}^4\right) \\ & + \frac{\varphi_{i,3}^4}{4h_{i,2}^4} - \frac{1}{2}\frac{\varphi_{i,2}^6}{\left(K_{a,i,2}^4 - \varphi_{i,2}^4\right)^2} - \frac{\varphi_{i,2}^4}{4h_{i,1}^4} - \tilde{\vartheta}_{i,2}^{\mathrm{T}}\dot{\hat{\vartheta}}_{i,2}, \end{aligned} \tag{29}$$

where $M_{i,2}=\frac{\left(3K_{a,i,2}^4+\varphi_{i,2}^4\right)^2\varphi_{i,2}}{2\left(K_{a,i,2}^4-\varphi_{i,2}^4\right)^3}+\frac{3\left(h_{i,2}^{\frac{4}{3}}+1\right)\varphi_{i,2}}{4\left(K_{a,i,2}^4-\varphi_{i,2}^4\right)^{\frac{1}{3}}}+\frac{\varphi_{i,2}}{4}\left(\frac{\partial\alpha_{i,1}}{\partial x_{i,1}}\right)^4+\Phi_{i,2}-\nabla\alpha_{i,1}+\frac{\varphi_{i,2}^3}{2\left(K_{a,i,2}^4-\varphi_{i,2}^4\right)}+\frac{\varphi_{i,2}}{4h_{i,1}^4}$ and $h_{i,2}$ is a positive constant.

Similarly, $M_{i,2}$ cannot be directly used in the design of the controller. According to Lemma 3, $M_{i,2}$ can be approximated by $\vartheta_{i,2}^{\mathrm{T}}P_{m_{i,2}}$. Especially, for $\forall\varepsilon_{i,2}>0$, the following inequality holds

$$M_{i,2}\left(\boldsymbol{\varphi}_{i,2}\right)=\vartheta_{i,2}^{\mathrm{T}}P_{m_{i,2}}\left(\boldsymbol{\varphi}_{i,2}\right)+\delta_{i,2}\left(\boldsymbol{\varphi}_{i,2}\right), \tag{30}$$

where $\boldsymbol{\varphi}_{i,2}=\left[\varphi_{i,1},\varphi_{i,2}\right]^{\mathrm{T}}$ denotes the input vector and approximation error $\delta_{i,2}\left(\boldsymbol{\varphi}_{i,2}\right)$ satisfies $\left|\delta_{i,2}\left(\boldsymbol{\varphi}_{i,2}\right)\right|\leq\varepsilon_{i,2}$.

Then, based on Young's Inequality, the following inequality is holds

$$\frac{\varphi_{i,2}^3}{K_{a,i,2}^4-\varphi_{i,2}^4}M_{i,2}\leq\frac{\varphi_{i,2}^3}{K_{a,i,2}^4-\varphi_{i,2}^4}\vartheta_{i,2}^{\mathrm{T}}P_{m_{i,2}}+\frac{1}{2}\frac{\varphi_{i,2}^6}{\left(K_{a,i,2}^4-\varphi_{i,2}^4\right)^2}+\frac{1}{2}\varepsilon_{i,2}^2. \tag{31}$$

Combining (29), (30) with (31), the following inequality yields

$$L\Gamma_{i,2}\leq L\Gamma_{i,1}+\frac{\varphi_{i,2}^3}{K_{a,i,2}^4-\varphi_{i,2}^4}\left(\alpha_{i,2}+\vartheta_{i,2}^{\mathrm{T}}P_{m_{i,2}}\right)+\frac{N}{4}\sum_{k=1}^{N}\left(y_k^4\bar{\mathrm{H}}_{i,2,k}^4+y_k^4\bar{\Psi}_{i,2,k}^4\right)+\frac{\varphi_{i,3}^4}{4h_{i,2}^4}-\tilde{\vartheta}_{i,2}^{\mathrm{T}}\dot{\hat{\vartheta}}_{i,2}+\frac{1}{2}\varepsilon_{i,2}^2. \tag{32}$$

According to (32), designed the second virtual control signal $\alpha_{i,2}$ as follows

$$\alpha_{i,2}=-b_{i,2}\varphi_{i,2}-\hat{\vartheta}_{i,2}^{\mathrm{T}}P_{m_{i,2}}, \tag{33}$$

where $b_{i,2}>0$ is a constant.

Substituting the virtual control signal (33) into (32), the following inequality can be established

$$\begin{aligned}L\Gamma_{i,2}\leq L\Gamma_{i,1}&-\frac{b_{i,2}\varphi_{i,2}^4}{K_{a,i,2}^4-\varphi_{i,2}^4}+\tilde{\vartheta}_{i,2}^{\mathrm{T}}\left(\frac{\varphi_{i,2}^3}{K_{a,i,2}^4-\varphi_{i,2}^4}P_{m_{i,2}}-\dot{\hat{\vartheta}}_{i,2}\right)\\&+\frac{N}{4}\sum_{k=1}^{N}\left(y_k^4\bar{\mathrm{H}}_{i,2,k}^4+y_k^4\bar{\Psi}_{i,2,k}^4\right)+\frac{\varphi_{i,3}^4}{4h_{i,2}^4}-\frac{\varphi_{i,2}^4}{4h_{i,1}^4}+\frac{\varepsilon_{i,2}^2}{2}.\end{aligned} \tag{34}$$

In view of (34), constructed the second adaptive law $\dot{\hat{\vartheta}}_{i,2}$ as follows

$$\dot{\hat{\vartheta}}_{i,2}=-\mu_{i,2}\hat{\vartheta}_{i,2}+\frac{\varphi_{i,2}^3}{K_{a,i,2}^4-\varphi_{i,2}^4}P_{m_{i,2}}, \tag{35}$$

where $\mu_{i,2}>0$ is a constant.

Then, substituting (35) into (34), the following inequality is holds

$$L\Gamma_{i,2}\leq\Xi_{i,j}^2+\frac{\varphi_{i,3}^4}{4h_{i,2}^4}+\frac{N}{4}\sum_{k=1}^{N}\left(w_{i,1,e}^2y_k^4\bar{\Psi}_{i,1,k}^4+y_k^4\bar{\Psi}_{i,2,k}^4\right)-G_i, \tag{36}$$

where $\Xi_{i,j}^2=\sum_{j=1}^{2}\left(\frac{-b_{i,j}\varphi_{i,j}^4}{K_{a,i,j}^4-\varphi_{i,j}^4}+\frac{N}{4}\sum_{k=1}^{N}y_k^4\bar{\mathrm{H}}_{i,j,k}^4+\mu_{i,j}\tilde{\vartheta}_{i,j}^{\mathrm{T}}\hat{\vartheta}_{i,j}+\frac{\varepsilon_{i,j}^2}{2}\right)$.

Step i,s $(3\leq s\leq n_{i-1})$: Constructing the following Lyapunov function as follows

$$\Gamma_{i,s}=L\Gamma_{i,s-1}+\frac{1}{4}\log\frac{K_{a,i,s}^4}{K_{a,i,s}^4-\varphi_{i,s}^4}+\frac{1}{2}\tilde{\vartheta}_{i,s}^{\mathrm{T}}\tilde{\vartheta}_{i,s}, \tag{37}$$

where $K_{a,i,s} = B_{i,s} - \gamma_{s-1}$ with γ_{s-1} is a positive constant, $\tilde{\vartheta}_{i,s} = \vartheta_{i,s} - \hat{\vartheta}_{i,s}$ represents the parameter error vector, and $\hat{\vartheta}_{i,s}$ is the estimation of $\vartheta_{i,s}$.

According to (5) and (13), the following equation can be obtained

$$dx_{i,s} = \left(x_{i,s+1} + \Phi_{i,s} + \mathrm{H}_{i,s} - \nabla\alpha_{i,s-1}\right) dt + F_{i,s}^{\mathrm{T}} d\omega, \tag{38}$$

where $\nabla\alpha_{i,s-1} = \sum_{j=1}^{s-1}\left(\frac{\partial\alpha_{i,s-1}}{\partial x_{i,j}}\left(x_{i,j+1} + \Phi_{i,j} + \mathrm{H}_{i,j}\right) + \frac{\partial\alpha_{i,s-1}}{\partial\hat{\vartheta}_{i,j}}\dot{\hat{\vartheta}}_{i,j}\right) + \sum_{j=0}^{s-1}\frac{\partial\alpha_{i,s-1}}{\partial y_{r,i}^{(j)}} y_{r,i}^{(j+1)} + \frac{1}{2}\sum_{p,q=1}^{s-1}\frac{\partial^2\alpha_{i,s-1}}{\partial x_{i,p}x_{i,q}}\Psi_{i,p}^{\mathrm{T}}\Psi_{i,q}$ and $F_{i,s} = \Psi_{i,n} - \sum_{j=1}^{s-1}\frac{\partial\alpha_{i,s-1}}{\partial x_{i,j}}\Psi_{i,j}$.

Repeating the design process in Step 2, the virtual control signal $\alpha_{i,s}$ and control law $\dot{\hat{\vartheta}}_{i,s}$ can be designed as follows

$$\alpha_{i,s} = -b_{i,s}\varphi_{i,s} - \hat{\vartheta}_{i,s}^{\mathrm{T}} P_{m_{i,s}}, \tag{39}$$

$$\dot{\hat{\vartheta}}_{i,s} = -\mu_{i,s}\hat{\vartheta}_{i,s} + \frac{\varphi_{i,s}^3}{K_{a,i,s}^4 - \varphi_{i,s}^4} P_{m_{i,s}}, \tag{40}$$

where $b_{i,s} > 0$ and $\mu_{i,s} > 0$ are design constants.

Similarly, we can get the derivative of $\Gamma_{i,s}$ with respect to t as follows

$$L\Gamma_{i,s} \le \Xi_{i,j}^s + \frac{\varphi_{i,s}^4}{4h_{i,s-1}^4} + \frac{N}{4}\sum_{k=1}^{N} w_{i,1,e}^2 y_k^4 \overline{\Psi}_{i,1,k}^4 + \frac{N}{4}\sum_{k=1}^{N}\sum_{j=2}^{s} y_k^4 \overline{\Psi}_{i,j,k}^4 - G_i, \tag{41}$$

with $\Xi_{i,j}^s = \sum_{j=1}^{s}\left(\frac{-b_{i,j}\varphi_{i,j}^4}{K_{a,i,j}^4 - \varphi_{i,j}^4} + \frac{N}{4}\sum_{k=1}^{N} y_k^4 \bar{\mathrm{H}}_{i,j,k}^4 + \mu_{i,j}\tilde{\vartheta}_{i,j}^{\mathrm{T}}\hat{\vartheta}_{i,j} + \frac{\epsilon_{i,j}^2}{2}\right)$ and $h_{i,s-1} > 0$ is a design constant.

Step i, n_i: Constructing the following Lyapunov function as

$$\Gamma_{i,n_i} = \Gamma_{i,n_i-1} + \frac{1}{4}\log\frac{K_{a,i,n_i}^4}{K_{a,i,n_i}^4 - \varphi_{i,n_i}^4} + \frac{1}{2}\tilde{\vartheta}_{i,n_i}^{\mathrm{T}}\tilde{\vartheta}_{i,n_i}, \tag{42}$$

where $K_{a,i,n_i} = B_{i,n_i} - \gamma_{n_i-1}$ with γ_{n_i-1} is a positive constant, $\tilde{\vartheta}_{i,n_i} = \vartheta_{i,n_i} - \hat{\vartheta}_{i,n_i}$ represents the parameter error vector, and $\hat{\vartheta}_{i,n_i}$ is the estimation of ϑ_{i,n_i}.

Calculating the derivative of Γ_{i,n_i} with respect to time t, we have

$$\begin{aligned} L\Gamma_{i,n_i} = {} & L\Gamma_{i,n_i-1} + \frac{\varphi_{i,n_i}^3}{K_{a,i,n_i}^4 - \varphi_{i,n_i}^4}\left(\Theta_i(v_i) + \eta_i v_i + \Phi_{i,n_i} + \mathrm{H}_{n_i} - \nabla\alpha_{i,n_i-1}\right) \\ & + \frac{\varphi_{i,n_i}^2\left(3K_{a,i,n_i}^4 + \varphi_{i,n_i}^4\right)}{2\left(K_{a,i,n_i}^4 - \varphi_{i,n_i}^4\right)^2}\left\|F_{i,n_i}\right\|^2 - \tilde{\vartheta}_{i,n_i}^{\mathrm{T}}\dot{\hat{\vartheta}}_{i,n_i}, \end{aligned} \tag{43}$$

where $\nabla\alpha_{i,n_i-1} = \sum_{j=1}^{n_i-1}\left(\frac{\partial\alpha_{i,n_i-1}}{\partial x_{i,j}}\left(x_{i,j+1} + \Phi_{i,j} + \mathrm{H}_{i,j}\right) + \frac{\partial\alpha_{i,n_i-1}}{\partial\hat{\vartheta}_{i,j}}\dot{\hat{\vartheta}}_{i,j}\right) + \sum_{j=0}^{n_i-1}\frac{\partial\alpha_{i,n_i-1}}{\partial y_{r,i}^{(j)}} y_{r,i}^{(j+1)} + \frac{1}{2}\sum_{p,q=1}^{n_i-1}\frac{\partial^2\alpha_{i,n_i-1}}{\partial x_{i,p}x_{i,q}}\Psi_{i,p}^{\mathrm{T}}\Psi_{i,q}$ and $F_{i,n_i} = \Psi_{i,n} - \sum_{j=1}^{n_i-1}\frac{\partial\alpha_{i,n_i-1}}{\partial x_{i,j}}\Psi_{i,j}$.

By employing Assumption 2 and Remark 2, the following inequality can be obtained

$$\frac{\varphi_{i,n_i}^3}{K_{a,i,n_i}^4 - \varphi_{i,n_i}^4}\Theta_i(v_i) \le \frac{3\xi_i^{\frac{4}{3}}\varphi_{i,n_i}^4}{4\left(K_{a,i,n_i}^4 - \varphi_{i,n_i}^4\right)^{\frac{4}{3}}} + \frac{1}{4\xi_i^4}\overline{\Theta}_i^4, \tag{44}$$

where $\xi_i > 0$ is a constant.

Substituting (44) in (43), we have

$$L\Gamma_{i,n_i} \le L\Gamma_{i,n_i-1} + \frac{\varphi_{i,n_i}^3\left(\eta_i v_i + \mathrm{M}_{i,n_i}\right)}{K_{a,i,n_i}^4 - \varphi_{i,n_i}^4} - \frac{\varphi_{i,n_i}^4}{4h_{i,n_i-1}^4} - \tilde{\boldsymbol{\vartheta}}_{i,n_i}^{\mathrm{T}}\dot{\hat{\boldsymbol{\vartheta}}}_{i,n_i} + \frac{N}{4}\sum_{k=1}^{N}\left(y_k^4\overline{\Psi}_{i,n_i,k}^4 + y_k^4\overline{\mathrm{H}}_{i,n_i,k}^4\right) - \frac{\varphi_{i,n_i}^6}{2\left(K_{a,i,n_i}^4 - \varphi_{i,n_i}^4\right)^2} + \frac{1}{4\xi_i^4}\overline{\Theta}_i^4, \tag{45}$$

where $\mathrm{M}_{i,n_i} = \Phi_{i,n_i} + \frac{3\varphi_{i,n_i}\left(1+\xi_i^{\frac{4}{3}}\right)}{4\left(K_{a,i,n_i}^4-\varphi_{i,n_i}^4\right)^{\frac{1}{3}}} + \frac{n_i\left(3K_{a,i,n_i}^4+\varphi_{i,n_i}^4\right)^2\varphi_{i,n_i}}{4\left(K_{a,i,n_i}^4-\varphi_{i,n_i}^4\right)^3} + \frac{n_i\varphi_{i,n_i}}{4}\left(\sum_{b=1}^{n_i-1}\frac{\partial\alpha_{n_i-1}}{\partial x_{i,b}}\right)^4 + \frac{\varphi_{i,n_i}}{4h_{i,n_i-1}^4} + \frac{\varphi_{i,n_i}^3}{2K_{a,i,n_i}^4-\varphi_{i,n_i}^4} - \nabla\alpha_{i,n_i-1}$ and h_{i,n_i-1} is a positive constant.

According to Lemma 3, the unknown nonlinear function M_{i,n_i} can be approximated by an MTN with any $\varepsilon_{i,n_i} > 0$. In other words, there is

$$M_{i,n_i}\left(\boldsymbol{\varphi}_{i,n_i}\right) = \boldsymbol{\vartheta}_{i,n_i}^{\mathrm{T}}P_{m_{i,n_i}}\left(\boldsymbol{\varphi}_{i,n_i}\right) + \delta_{i,n_i}\left(\boldsymbol{\varphi}_{i,n_i}\right), \tag{46}$$

where $\boldsymbol{\varphi}_{i,n_i} = \left[\varphi_{i,1}, \varphi_{i,2}, \ldots, \varphi_{i,n_i}\right]^{\mathrm{T}}$ denotes the input vector and approximation error $\delta_{i,n_i}\left(\boldsymbol{\varphi}_{i,n_i}\right)$ satisfies $\left|\delta_{i,n_i}\left(\boldsymbol{\varphi}_{i,n_i}\right)\right| \le \varepsilon_{i,n_i}$.

Then, based on Young's Inequality, the following inequality is holds

$$\frac{\varphi_{i,n_i}^3}{K_{a,i,n_i}^4 - \varphi_{i,n_i}^4}M_{i,n_i} \le \frac{\varphi_{i,n_i}^3}{K_{a,i,n_i}^4 - \varphi_{i,n_i}^4}\boldsymbol{\vartheta}_{i,n_i}^{\mathrm{T}}P_{m_{i,n_i}} + \frac{1}{2}\frac{\varphi_{i,n_i}^6}{\left(K_{a,i,n_i}^4 - \varphi_{i,n_i}^4\right)^2} + \frac{1}{2}\varepsilon_{i,n_i}^2. \tag{47}$$

Substituting (47) into (45), the following inequality is established

$$L\Gamma_{i,n_i} \le L\Gamma_{i,n_i-1} + \frac{\varphi_{i,n_i}^3}{K_{a,i,n_i}^4 - \varphi_{i,n_i}^4}\left(\eta_i v_i + \boldsymbol{\vartheta}_{i,n_i}^{\mathrm{T}}P_{m_{i,n_i}}\right) - \frac{\varphi_{i,n_i}^4}{4h_{i,n_i-1}^4} - \tilde{\boldsymbol{\vartheta}}_{i,n_i}^{\mathrm{T}}\dot{\hat{\boldsymbol{\vartheta}}}_{i,n_i} + \frac{N}{4}\sum_{k=1}^{N}\left(y_k^4\overline{\Psi}_{i,n_i,k}^4 + y_k^4\overline{\mathrm{H}}_{i,n_i,k}^4\right) + \frac{1}{2}\varepsilon_{i,n_i}^2 + \frac{1}{4\xi_i^4}\overline{\Theta}_i^4. \tag{48}$$

According to (48), designed the actual input signal v_i as follows

$$v_i = -\frac{1}{\sigma_{i,1}}\left(b_{i,n_i}\left|\varphi_{i,n_i}\right| + \left|\hat{\boldsymbol{\vartheta}}_{i,n_i}^{\mathrm{T}}P_{m_{i,n_i}}\right|\right)\mathrm{sign}\left(\varphi_{i,n_i}\right), \tag{49}$$

where $b_{i,n_i} > 0$ is a design constant.

Substituting the actual input signal (49) into (48), we have

$$L\Gamma_{i,n_i} \le L\Gamma_{i,n_i-1} + \tilde{\boldsymbol{\vartheta}}_{i,n_i}^{\mathrm{T}}\left(\frac{\varphi_{i,n_i}^3}{K_{a,i,n_i}^4 - \varphi_{i,n_i}^4}P_{m_{i,n_i}} - \dot{\hat{\boldsymbol{\vartheta}}}_{i,n_i}\right) - \frac{\varphi_{i,n_i}^4}{4h_{i,n_i-1}^4} + \frac{N}{4}\sum_{k=1}^{N}y_k^4\overline{\Psi}_{i,n_i,k}^4 + \frac{N}{4}\sum_{k=1}^{N}y_k^4\overline{\mathrm{H}}_{i,n_i,k}^4 + \frac{1}{2}\varepsilon_{i,n_i}^2 + \frac{1}{4\xi_i^4}\overline{\Theta}_i^4. \tag{50}$$

According to (50), design the n_ith adaptive law as follows

$$\dot{\hat{\boldsymbol{\vartheta}}}_{i,n_i} = -\mu_{i,n_i}\hat{\boldsymbol{\vartheta}}_{i,n_i} + \frac{\varphi_{i,n_i}^3}{K_{a,i,n_i}^4 - \varphi_{i,n_i}^4}P_{m_{i,n_i}}, \tag{51}$$

where $\mu_{i,n_i} > 0$ is a constant.

By combining (41), (50), and (51), the following inequality can be obtained

$$L\Gamma_{i,n_i} \le \Xi_{i,j}^{n_i} + \frac{N}{4}\sum_{k=1}^{N} w_{i,1,e}^2 y_k^4 \overline{\Psi}_{i,1,k}^4 + \frac{N}{4}\sum_{j=2}^{n_i}\sum_{k=1}^{N} y_k^4 \overline{\Psi}_{i,j,k}^4 + \frac{1}{4\xi_i^4}\overline{\Theta}_i^4 - G_i, \tag{52}$$

with $\Xi_{i,j}^{n_i} = \sum_{j=1}^{n_i}\left(\frac{-b_{i,j}\varphi_{i,j}^4}{K_{a,i,j}^4 - \varphi_{i,j}^4} + \frac{N}{4}\sum_{k=1}^{N} y_k^4 \bar{\mathrm{H}}_{i,j,k}^4 + \mu_{i,j}\tilde{\vartheta}_{i,j}^{\mathrm{T}}\hat{\vartheta}_{i,j} + \frac{\varepsilon_{i,j}^2}{2}\right)$.

So far, the controller design is completed, the design process of the above control scheme is shown in Figure 1. The main results of this paper will be given by the following Theorem.

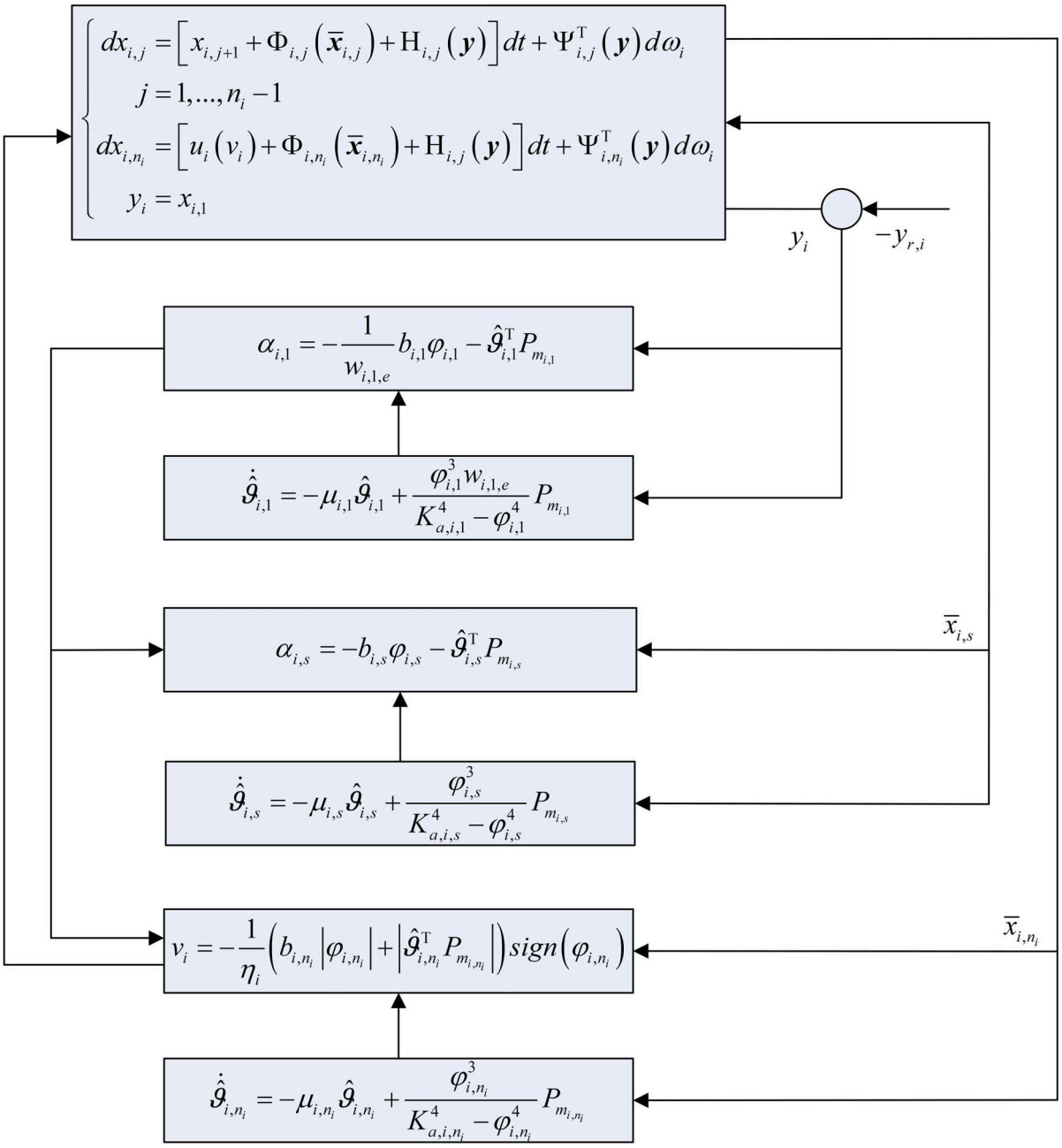

FIGURE 1 The control system block diagram.

3.2 | Stability analysis

Theorem 1. *Under the conditions of Assumptions 1–3, consider the closed-loop system consisting of the large-scale stochastic nonlinear system (5), the virtual control signals (23), (33), (39), the actual input (49), with the adaptive laws (25), (35), (40) and (51). Then for arbitrary bounded initial conditions, the following conclusions are true:*

(1) All signals of the closed-loop system are SGUUB in probability.
(2) All states $x_{i,j}, i = 1, \dots, N; j = 1, \dots, n_i$ are not violating the given constraint bounds.
(3) All the desired reference signal $y_{r,i}, i = 1, 2, \dots, N$ are well tracked by the output y_i of ith subsystem, respectively. Further more, the tracking error $e_i = y_i - y_{r,i}$ converges to the predetermined allowable range.

Proof. According to the above backstepping process, constructing the following Lyapunov function for the closed-loop system

$$\Gamma = \frac{1}{4}\sum_{i=1}^{N}\sum_{j=1}^{n_i}\log\frac{K_{a,i,j}^4}{K_{a,i,j}^4 - \varphi_{i,j}^4} + \frac{1}{2}\sum_{i=1}^{N}\sum_{j=1}^{n_i}\tilde{\vartheta}_{i,j}^{\mathrm{T}}\tilde{\vartheta}_{i,j}. \tag{53}$$

According to (52), the derivative of Γ can be calculated as follows

$$\begin{aligned} L\Gamma \le & \sum_{i=1}^{N}\sum_{j=1}^{n_i}\left(-b_{i,j}\frac{\varphi_{i,j}^4}{K_{a,i,j}^4 - \varphi_{i,j}^4} + \frac{N}{4}\sum_{k=1}^{N}y_k^4\overline{\mathrm{H}}_{i,j,k}^4 + \mu_{i,j}\tilde{\vartheta}_{i,j}^{\mathrm{T}}\hat{\vartheta}_{i,j} + \frac{1}{2}\varepsilon_{i,j}^2\right) + \frac{N}{4}\sum_{i=1}^{N}\sum_{k=1}^{N}w_{i,1,e}^2y_k^4\overline{\Psi}_{i,1,k}^4 \\ & + \frac{N}{4}\sum_{i=1}^{N}\sum_{j=2}^{n_i}\sum_{k=1}^{N}y_k^4\overline{\Psi}_{i,j,k}^4 + \sum_{i=1}^{N}\frac{1}{4\xi_i^4}\overline{\Theta}_i^4 - \sum_{i=1}^{N}G_i, \end{aligned} \tag{54}$$

where $b_{i,j}$, $\mu_{i,j}$, and ξ_i are positive design constants for $i = 1, 2, \dots, N, j = 1, 2, \dots, n_i$.

According to Young's Inequality, the term $\sum_{i=1}^{N}\sum_{j=1}^{n_i}\mu_{i,j}\tilde{\vartheta}_{i,j}^{\mathrm{T}}\hat{\vartheta}_{i,j}$ in (54) can be transformed as follows

$$\sum_{i=1}^{N}\sum_{j=1}^{n_i}\mu_{i,j}\tilde{\vartheta}_{i,j}^{\mathrm{T}}\hat{\vartheta}_{i,j} \le -\frac{1}{2}\sum_{i=1}^{N}\sum_{j=1}^{n_i}\mu_{i,j}\tilde{\vartheta}_{i,j}^{\mathrm{T}}\tilde{\vartheta}_{i,j} + \frac{1}{2}\sum_{i=1}^{N}\sum_{j=1}^{n_i}\mu_{i,j}\vartheta_{i,j}^{\mathrm{T}}\vartheta_{i,j}. \tag{55}$$

Then, substituting (55) into (54), and according to Lemma 2, we have

$$\begin{aligned} L\Gamma \le & -\sum_{i=1}^{N}\sum_{j=1}^{n_i}\left(b_{i,j}\log\frac{K_{a,i,1}^4}{K_{a,i,j}^4 - \varphi_{i,j}^4} + \frac{1}{2}\mu_{i,j}\tilde{\vartheta}_{i,j}^{\mathrm{T}}\tilde{\vartheta}_{i,j}\right) + \sum_{i=1}^{N}\sum_{j=1}^{n_i}\left(\frac{1}{2}\varepsilon_{i,j}^4 + \frac{1}{2}\mu_{i,j}\vartheta_{i,j}^{\mathrm{T}}\vartheta_{i,j}\right) - \sum_{i=1}^{N}G_i + \sum_{i=1}^{N}\frac{1}{4\xi_i^4}\overline{\Theta}_i^4 \\ & + \frac{N}{4}\sum_{i=1}^{N}\sum_{k=1}^{N}\left(w_{i,1,e}^2y_k^4\overline{\Psi}_{i,1,k}^4 + \sum_{j=1}^{n_i}y_k^4\overline{\mathrm{H}}_{i,j,k}^4 + \sum_{j=2}^{n_i}y_k^4\overline{\Psi}_{i,j,k}^4\right). \end{aligned} \tag{56}$$

Choosing the smooth nonnegative function candidate $\chi\left(\varphi_{i,1}^2\right)\varphi_{i,1}^4$ satisfies the following inequality

$$\frac{N}{4}\sum_{k=1}^{N}\left(w_{i,1,e}^2y_k^4\overline{\Psi}_{i,1,k}^4 + \sum_{j=1}^{n_i}y_k^4\overline{\mathrm{H}}_{i,j,k}^4 + \sum_{j=2}^{n_i}y_k^4\overline{\Psi}_{i,j,k}^4\right) - G_i \le 0. \tag{57}$$

Combining (56) with (57), the following inequality can be obtained

$$L\Gamma \leq -\sum_{i=1}^{N}\sum_{j=1}^{n_i}\left(b_{i,j}\log\frac{K_{a,i,1}^4}{K_{a,i,j}^4-\varphi_{i,j}^4}+\frac{1}{2}\mu_{i,j}\tilde{\boldsymbol{\vartheta}}_{i,j}^{\mathrm{T}}\tilde{\boldsymbol{\vartheta}}_{i,j}\right)+\sum_{i=1}^{N}\sum_{j=1}^{n_i}\left(\frac{1}{2}\epsilon_{i,j}^4+\frac{1}{2}\mu_{i,j}\boldsymbol{\vartheta}_{i,j}^{\mathrm{T}}\boldsymbol{\vartheta}_{i,j}+\frac{1}{4\xi_i^4}\overline{\Theta}_i^4\right). \tag{58}$$

Let $\lambda=\min\{\lambda_1,\lambda_2,\ldots,\lambda_N\}$ and $\tau=\sum_{i=1}^{N}\sum_{j=1}^{n_i}\left(\frac{1}{2}\epsilon_{i,j}^4+\frac{1}{2}\mu_{i,j}\boldsymbol{\vartheta}_{i,j}^{\mathrm{T}}\boldsymbol{\vartheta}_{i,j}+\frac{1}{4\xi_i^4}\overline{\Theta}_i^4\right)$ with $\lambda_i=\min\left\{4b_{i,j},2\mu_{i,j}|i=1,\ldots,N,j=1,\ldots,n_i\right\}$. The inequality (58) can be rewritten as follows

$$L\Gamma \leq -\lambda\Gamma+\tau. \tag{59}$$

Using Lemma 1 and (59), the following inequality is holds

$$\frac{d\left(E\left[\Gamma\right]\right)}{dt}\leq d\left(L\left[\Gamma\right]\right)\leq\lambda E\left[\Gamma\right]+\tau. \tag{60}$$

Based on (60) and Definition 2, the following inequality can be obtained

$$0\leq E\left[\Gamma\right]\leq\Gamma\left(0\right)e^{-\lambda t}+\frac{\lambda}{\tau},\quad\forall t>0. \tag{61}$$

That is to say, the $E\left[\Gamma\right]$ is bounded by $\frac{\lambda}{\tau}$. Further more, it can be concluded that

$$E\left[\left|\varphi_{i,1}\right|^4\right]\leqslant 4E\left[\Gamma\right]\leqslant 4\left[e^{-\lambda t}\left[\Gamma\left(0\right)\right]+\frac{\lambda}{\tau}\right]. \tag{62}$$

Further, we have $\left|\varphi_{i,j}\right|\leqslant\varphi_{i,j}\sqrt[4]{1-e^{-4\left(\Gamma(0)+\frac{\lambda}{\tau}\right)}}$, so the tracking error $\left|y_i-y_{r,i}\right|$ can converge to an arbitrary neighborhood of the origin, and its radius of convergence depends on the values of λ and τ. This also shows that the PPC was successfully achieved.

It is clear from the above discussion that $\varphi_{i,j}$ is bounded. On the one hand, for $j=1$, $\varphi_{i,1}=x_{i,1}-y_{r,i}$ and $|y_{r,i}|\leq\gamma_{i,0}\leq B_{i,1}$, according to the absolute value inequality, we have $\left|x_{i,1}\right|\leq\left|\varphi_{i,1}\right|+\left|y_{r,i}\right|\leq K_{a,i,1}+\gamma_{i,0}$, that is to say, $\left|x_{i,1}\right|$ is bounded. It is already known from the backstepping process that $K_{a,i,1}=B_{i,1}-\gamma_{i,0}$, then the state $x_{i,1}$ satisfies the constraint $\left|x_{i,1}\right|\leq B_{i,1}$. As both $\varphi_{i,1}$ and $x_{i,1}$ are bounded, we can get $\alpha_{i,1}$ is bounded according to (23). Then, let $\left|\alpha_{i,j-1}\right|\leq\gamma_{j-1}$. For $j=2,3,\ldots,n_i$, from the boundedness of $\varphi_{i,j}=x_{i,j}-\alpha_{i,j-1}$, $\varphi_{i,j}$ and $\alpha_{i,j-1}$, we can obtain $\left|x_{i,j}\right|\leq\left|\varphi_{i,j}\right|+\left|\alpha_{i,j-1}\right|\leq K_{a,i,1}+\gamma_{i,j-1}$, that is, $x_{i,j}$ is also bounded. Based on $K_{a,i,j}=B_{i,j}-\gamma_{i,j-1}$ and $\left|\alpha_{i,j-1}\right|\leq\gamma_{j-1}$, $\left|x_{i,j}\right|\leq B_{i,j}$ can be easily obtained. Thus, all states in the closed-loop system do not exceed the given constraints. On the other hand, according to (50), it is known that v_i is a function of $\varphi_{i,j}$ and $\hat{\boldsymbol{\vartheta}}_{i,j}$, we can determine the actual control signal v_i is bounded based on the boundedness of $\varphi_{i,j}$ and $\hat{\boldsymbol{\vartheta}}_{i,j}$. Therefore, we can conclude that all signals in the system are SGUUB in probability.

Therefore, all the conclusions proposed in Theorem 1 are proved. ∎

Remark 3. According to Theorem 1, the control strategy proposed in this paper successfully achieves the PPC. The transient performance is closely related to the initial condition selection, in which $w_{i,0}$ can be chosen based on the tracking error at the initial time. In practical application, the parameters, such as $w_{i,0}$, l_i, and $w_{i,\infty}$, should be properly chosen for achieving satisfactory control performance.

Remark 4. The aforementioned stability analysis shows that the control performance of system is strongly influenced not only by the initial conditions, but also by the design parameters chosen. The tracking performance can be dramatically enhanced by selecting the optimal design parameters. As shown by (62), the convergence speed will increase when τ becomes smaller or λ becomes larger. In other words, we can reduce τ by lowering $b_{i,j}$ and $\mu_{i,j}$ or increasing ξ_i, while we can increase λ by raising $\varepsilon_{i,j}$ and $\mu_{i,j}$. It is worth noting that by increasing $\mu_{i,j}$ to increase λ will lead to bigger τ, and by reducing $\mu_{i,j}$ to decrease τ will result in smaller λ, which makes the control objective more difficult to achieve. Therefore, in order to more successfully meet

the control objectives, the real engineering system should be carefully adjusted to select the most appropriate parameters.

4 | SIMULATION EXPERIMENT

In this section, a numerical example and a practical example are presented to verify the effectiveness and applicability of the proposed control strategy.

Example 1. In order to verify the effectiveness of the proposed method, consider the large-scale stochastic nonlinear system with two subsystems as follows

$$\begin{cases} dx_{1,1} = x_{1,2}dt \\ dx_{1,2} = \left(u_1\left(v_1\right) + x_{1,1}x_{1,2} + 0.1y_1 + 0.1y_2\right)dt + 0.1y_1 d\omega \\ y_1 = x_{1,1} \\ dx_{2,1} = x_{2,2}dt \\ dx_{2,2} = \left(u_2\left(v_2\right) + x_{2,1}x_{2,2} + 0.1y_1\right)dt + 0.1y_2 d\omega \\ y_2 = x_{2,1} \end{cases}. \tag{63}$$

The initial condition is selected as $x_{1,1}(0) = x_{1,2}(0) = x_{2,1}(0) = x_{2,2}(0) = 0.002$. The desired reference signals are selected as $y_{r,1} = 0.5\sin t$ and $y_{r,2} = 0.5\sin t$. The state constraints are set as $|x_{1,1}| \le 1.3$, $|x_{1,2}| \le 1$, $|x_{2,1}| \le 1.1$ and $|x_{2,2}| \le 1$. Moreover, the prescribed performance functions are $w_{11} = (4 - 0.15)e^{-0.8t} + 0.15$ and $w_{21} = (4 - 0.1)e^{-0.8t} + 0.1$.

In the simulation, the control structure of system (63) is designed as Theorem 1, and the design parameters are selected as $u_{1,\min} = u_{2,min} = -1.5$, $u_{1,\max} = u_{2,\max} = 2$, $\delta_{1,1} = 0.8$, $\delta_{1,2} = 1$, $\delta_{2,1} = 0.5$, $\delta_{2,2} = 1$, $K_{a,1,1} = 0.8$, $K_{a,1,2} = 0.5$, $K_{a,2,1} = 0.6$, $K_{a,2,2} = 0.5$, $\mu_{1,1} = 13$, $\mu_{1,2} = 15$, $\mu_{2,1} = \mu_{2,2} = 12$, $b_{1,1} = 9$, $b_{1,2} = 5$, $b_{2,1} = 13$, $b_{2,2} = 3$, $\sigma_{1,1} = 2$, $\sigma_{2,1} = 0.7$, respectively. The simulation results are shown in Figures 2–5.

Figure 2 illustrates that the output y_1, y_2 can closely track the desired reference signal $y_{r,1}$, $y_{r,2}$, and the tracking effect is also satisfactory. The trajectories of performance function $w_{1,1}$, $w_{2,1}$ and the tracking error $\varphi_{1,1}$, $\varphi_{2,1}$ are shown in Figure 3, it can be seen that the tracking errors can be converge to the prescribed performance constraint. Figure 4 depicts the response of the control inputs v_1, v_2 and the actual inputs u_1, u_2 when the system experiences input saturation, it can be clearly seen that the constructed controller can be easily applied to solve the input saturation problem in the system. The trajectories of states $x_{1,2}$ and $x_{2,2}$ are shown in Figure 5. As shown in Figures 2 and 5, all states in the closed-loop system do not violate its given constraints.

Example 2. In order to make the proposed control scheme more convincing, a class of three-stage inverted pendulum is employed, as stated in Reference 12, its system can be expressed as the large-scale stochastic nonlinear system in the following form

$$\begin{cases} dx_{1,1} = \left(x_{1,2} + \Phi_{1,1} + \mathrm{H}_{1,1}\right)dt + \Psi_{1,1}^{\mathrm{T}} d\omega \\ dx_{1,2} = \left(u_1 + \Phi_{1,2} + \mathrm{H}_{1,2}\right)dt + \Psi_{1,2}^{\mathrm{T}} d\omega \\ y_1 = x_{1,1} \\ dx_{2,1} = \left(x_{2,2} + \Phi_{2,1} + \mathrm{H}_{2,1}\right)dt + \Psi_{2,1}^{\mathrm{T}} d\omega \\ dx_{2,2} = \left(u_2 + \Phi_{2,2} + \mathrm{H}_{2,2}\right)dt + \Psi_{2,2}^{\mathrm{T}} d\omega \\ y_2 = x_{2,1} \\ dx_{3,1} = \left(x_{3,2} + \Phi_{3,1} + \mathrm{H}_{3,1}\right)dt + \Psi_{3,1}^{\mathrm{T}} d\omega \\ dx_{3,2} = \left(u_3 + \Phi_{3,2} + \mathrm{H}_{3,2}\right)dt + \Psi_{3,2}^{\mathrm{T}} d\omega \\ y_3 = x_{3,1} \end{cases}, \tag{64}$$

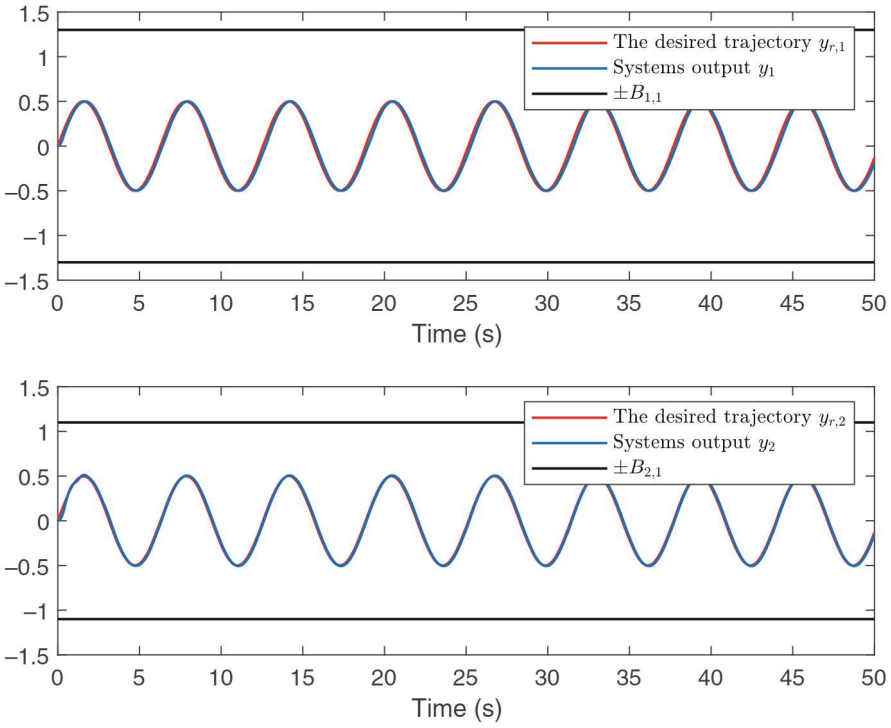

FIGURE 2 The trajectories of $y_1, y_{r,1}, y_2$ and $y_{r,2}$ of Example 1.

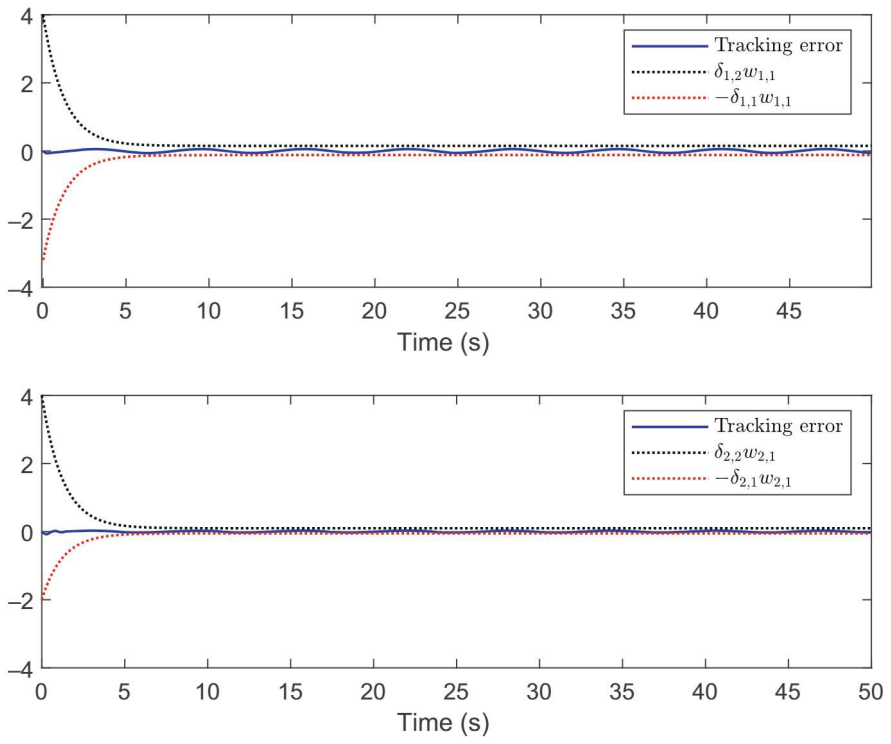

FIGURE 3 The trajectories of tracking errors and prescribed performance boundaries.

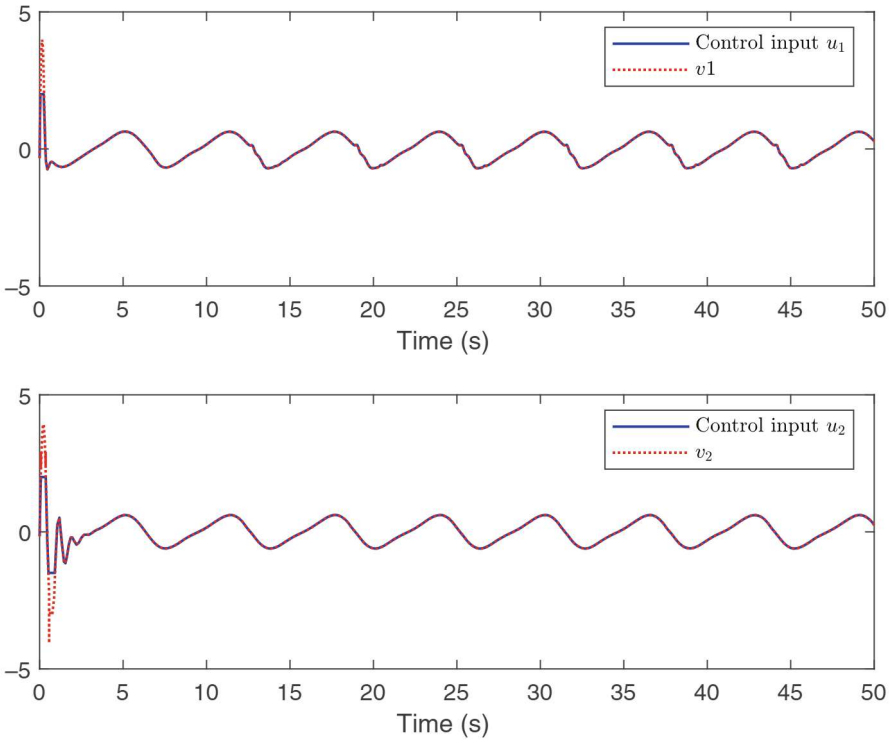

FIGURE 4 The trajectories of u_1, v_1, u_2 and v_2 of Example 1.

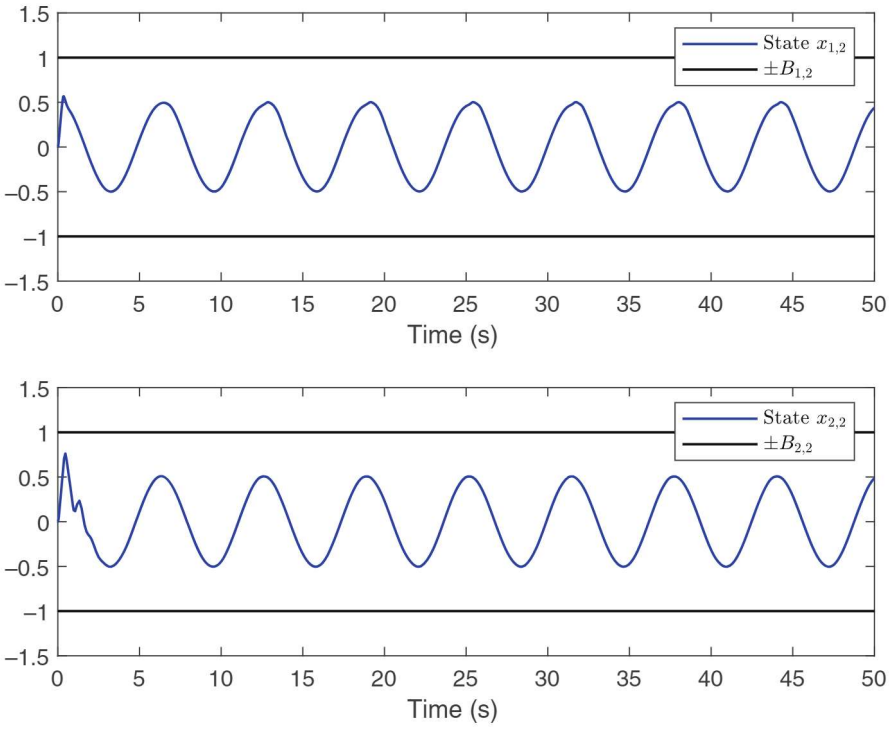

FIGURE 5 The trajectories of states $x_{1,2}$, $x_{2,2}$ and their constrained boundaries.

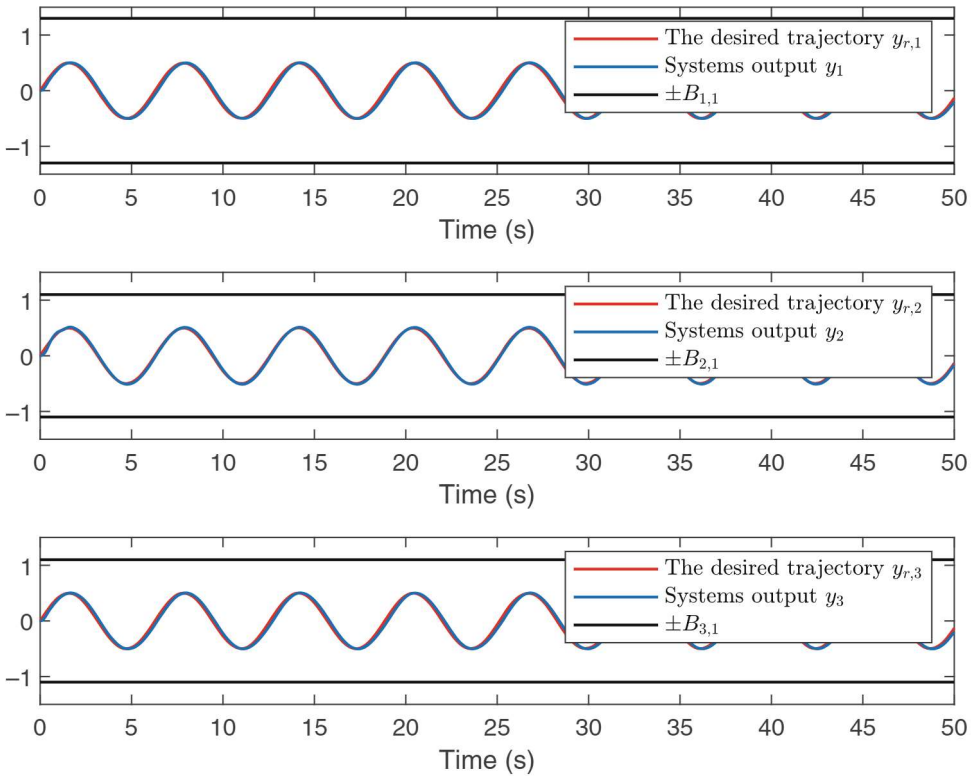

FIGURE 6 The trajectories of $y_1, y_{r,1}, y_2, y_{r,2}, y_3$, and $y_{r,3}$ of Example 2.

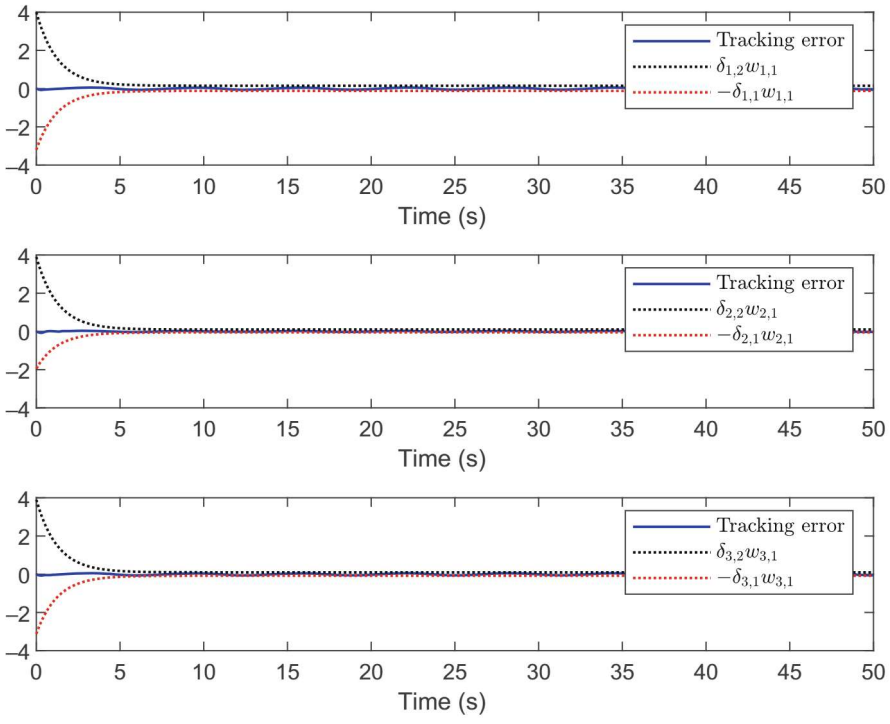

FIGURE 7 The trajectories of tracking errors and prescribed performance boundaries.

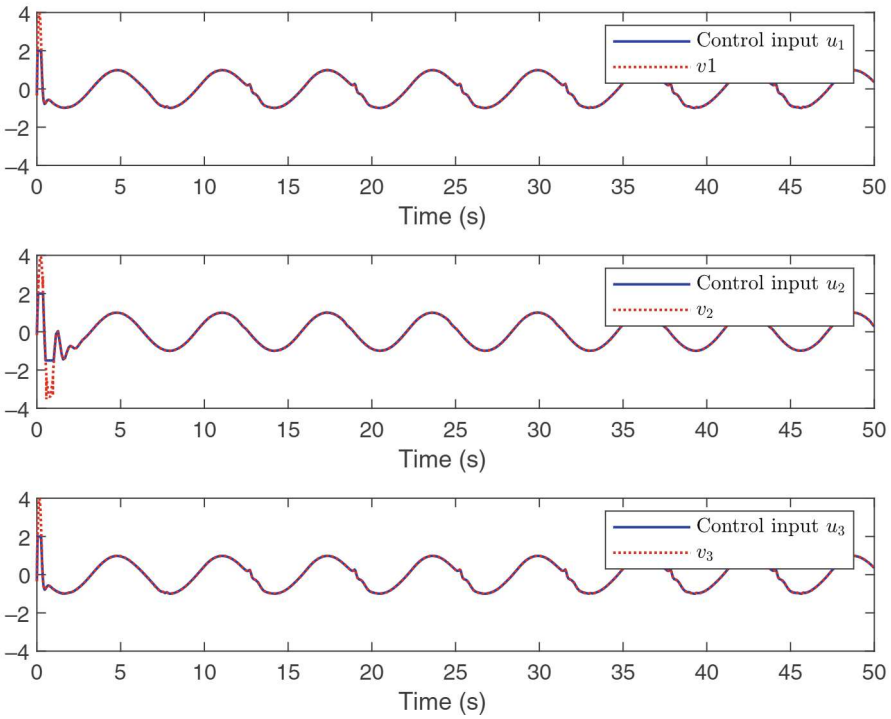

FIGURE 8 The trajectories of u_1, v_1, u_2, v_2, u_3, and v_3 of Example 2.

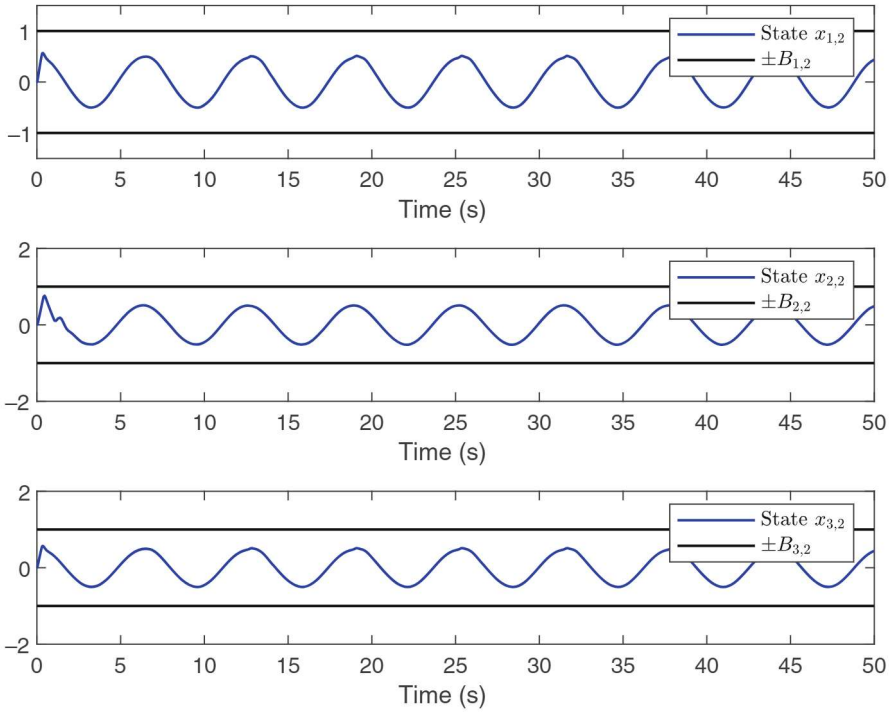

FIGURE 9 The trajectories of states $x_{1,2}$, $x_{2,2}$, $x_{3,2}$ and their constrained boundaries.

where $\Phi_{1,1} = \Phi_{2,1} = \Phi_{3,1} = 0$, $\Phi_{1,2} = \frac{g}{o}\sin x_{1,1}$, $\Phi_{2,2} = \frac{g}{o}\sin x_{2,1}$, $\Phi_{3,2} = \frac{g}{o}\sin x_{3,1}$, $\Psi_{1,1} = y_1 \sin y_1^3$, $\Psi_{2,1} = y_2 \sin y_2^3$, $\Psi_{3,1} = y_3 \sin y_3^3$, $\Psi_{1,2} = 0.5y_1$, $\Psi_{2,2} = 0.5\sin y_2^2$, $\Psi_{3,2} = 0.5y_3$, $\mathrm{H}_{1,1} = \mathrm{H}_{2,1} = \mathrm{H}_{3,1} = 0$, $\mathrm{H}_{1,2} = \frac{\upsilon_1 c^2}{\gamma_1 o^2}(\sin y_2 \cos y_2 - \sin y_1 \cos y_1)$, $\mathrm{H}_{2,2} = \frac{\upsilon_1 c^2}{\gamma_2 o^2}(\sin y_1 \cos y_1 - \sin y_2 \cos y_2) + \frac{\upsilon_2 c^2}{\gamma_2 o^2}(\sin y_3 \cos y_3 - \sin y_2 \cos y_2)$, and $\mathrm{H}_{3,2} = \frac{\upsilon_2 c^2}{\gamma_3 o^2}(\sin y_2 \cos y_2 - \sin y_3 \cos y_3)$, respectively.

The initial condition are selected as $x_{1,1}(0) = x_{1,2}(0) = 0.002$, $x_{2,1}(0) = x_{2,2}(0) = 0.002$ and $x_{3,1}(0) = x_{3,2}(0) = 0.002$. In the simulation, the reference signals are selected as $y_{r,1} = 0.5\sin t$, $y_{r,2} = 0.5\sin t$ and $y_{r,3} = 0.5\sin t$. The choice of control structure is the same as Theorem 1. The full states constraints are set as $|x_{1,1}| \le 1.3$, $|x_{1,2}| \le 1$, $|x_{2,1}| \le 1.1$, $|x_{2,2}| \le 1$, $|x_{3,1}| \le 1.3$ and $|x_{3,2}| \le 1$. Moreover, the prescribed performance functions are $w_{11} = (4 - 0.15)e^{-0.8t} + 0.15$, $w_{21} = (4 - 0.1)e^{-0.8t} + 0.1$ and $w_{31} = (4 - 0.15)e^{-0.8t} + 0.15$. All the design parameters are selected as $u_{1,\min} = u_{2,\min} = u_{3,\min} = -1.5$, $u_{1,\max} = u_{2,\max} = u_{3,\max} = 2$, $\delta_{1,1} = 0.8$, $\delta_{1,2} = 1$, $\delta_{2,1} = 0.5$, $\delta_{2,2} = 1$, $\delta_{3,1} = 0.8$, $\delta_{3,2} = 1$, $K_{a,1,1} = 0.8$, $K_{a,1,2} = 0.6$, $K_{a,2,1} = K_{a,2,2} = 0.5$, $K_{a,3,1} = 0.8$, $K_{a,3,2} = 0.6$, $\mu_{1,1} = 13$, $\mu_{1,2} = 15$, $\mu_{2,1} = \mu_{2,2} = 12$, $\mu_{3,1} = 13$, $\mu_{3,2} = 15$, $b_{1,1} = 9$, $b_{1,2} = 5$, $b_{2,1} = 13$, $b_{2,2} = 3$, $b_{3,1} = 9$, $b_{3,2} = 5$, $\sigma_{1,1} = 2$, $\sigma_{2,1} = 0.7$, $\sigma_{3,1} = 2$, respectively.

The simulation results of the system (64) are shown in Figures 6–9. According to Figures 6 and 7, the decentralized adaptive PPC strategy proposed in this paper can obtain a good tracking performance, and the system state obeys the full state constraints, meanwhile the control objectives can be successfully achieved. The feasibility and superiority of the control design approach developed in this research can be demonstrated using the above simulation results.

5 | CONCLUSION

In this paper, an adaptive decentralized controller integrating MTN, backstepping, BLFs, and PPC is designed for a class of large-scale stochastic nonlinear systems with input saturation and full state constraints. To deal with input saturation nonlinearity, a Gaussian error function is used, and BLFs are used to ensure full state constraints. The proposed control strategy can not only ensure that all signals of the closed-loop system are SGUUB in probability, but also realize the steady-state performance and transient performance of the system. Finally, two simulation examples demonstrate the effectiveness of the proposed control strategy. In comparison to traditional control methods, the finite-time control places more emphasis on real-time and fast characteristics. Therefore, our future work will focus on finite-time control of stochastic nonlinear systems with full state constraints.

ACKNOWLEDGMENTS

The authors would like to thank Editor-in-Chief, Associate Editor, and the anonymous reviewers for their insightful comments and valuable suggestions that are helpful for revising and improving our paper.

ORCID

Na Li https://orcid.org/0000-0002-7911-8903
Yang Du https://orcid.org/0000-0001-9503-6433
Yu-Qun Han https://orcid.org/0000-0002-9055-2954

REFERENCES

1. Zhang X, Lin Y. Nonlinear decentralized control of large-scale systems with strong interconnections. *Automatica*. 2014;50(9):2419-2423. doi:10.1016/j.automatica.2014.07.024
2. Zhou J. Decentralized adaptive control for large-scale time-delay systems with dead-zone input. *Automatica*. 2008;44(7):1790-1799. doi:10.1016/j.automatica.2007.10.037
3. Zhou J, Wen CY. Decentralized backstepping adaptive output tracking of interconnected nonlinear systems. *IEEE Trans Automat Control*. 2008;53(10):2378-2384. doi:10.1109/TAC.2008.2007524
4. Gao YF, Sun XM, Wang W. Decentralized backstepping adaptive output tracking of large-scale stochastic nonlinear systems. *Sci China Inform Sci*. 2017;60(12):120207. doi:10.1007/s11432-017-9142-3
5. Liu SJ, Zhang JF, Jiang ZP. Decentralized adaptive output-feedback stabilization for large-scale stochastic nonlinear systems. *Automatica*. 2007;43(2):238-251. doi:10.1016/j.automatica.2006.08.028
6. Jiang ZP, Repperger DW, Hill DJ. Decentralized nonlinear output-feedback stabilization with disturbance attenuation. *IEEE Trans Automat Control*. 2001;46(10):1623-1629. doi:10.1109/9.956061

7. Cui GZ, Wang Z, Zhuang GM, Li Z, Chu YM. Adaptive decentralized NN control of large-scale stochastic nonlinear time-delay systems with unknown dead-zone inputs. *Neurocomputing*. 2015;158:194-203. doi:10.1016/j.neucom.2015.01.048
8. Duan N, Min HF. Decentralized adaptive NN state-feedback control for large-scale stochastic high-order nonlinear systems. *Neurocomputing*. 2016;173:1412-1421. doi:10.1016/j.neucom.2015.09.013
9. Liu H, Li XH, Liu XP, Wang HQ. Backstepping-based decentralized bounded-H∞ adaptive neural control for a class of large-scale stochastic nonlinear systems. *J Franklin Inst*. 2019;356(15):8049-8079. doi:10.1016/j.jfranklin.2019.06.043
10. Tong SC, Sui S, Li YM. Adaptive fuzzy decentralized output stabilization for stochastic nonlinear large-scale systems with unknown control directions. *IEEE Trans Fuzzy Syst*. 2014;22(5):1365-1372. doi:10.1109/TFUZZ.2013.2291554
11. Wang LB, Wang HQ, Liu PX. Adaptive fuzzy finite-time decentralized control for large-scale stochastic nonlinear systems. *Int J Adapt Control Signal Proces*. 2021;35(10):2025-2039. doi:10.1002/acs.3306
12. Zhang TP, Xia XN. Decentralized adaptive fuzzy output feedback control of stochastic nonlinear large-scale systems with dynamic uncertainties. *Inform Sci*. 2015;315:17-38. doi:10.1016/j.ins.2015.04.002
13. Han YQ, Yan HS. Observer-based multi-dimensional Taylor network decentralised adaptive tracking control of large-scale stochastic nonlinear systems. *Int J Control*. 2020;93(7):1605-1618. doi:10.1080/00207179.2018.1521994
14. Han YQ. Adaptive tracking control of a class of nonlinear systems with unknown dead-zone output: a multi-dimensional Taylor network (MTN)-based approach. *Int J Control*. 2021;94(11):3161-3170. doi:10.1080/00207179.2020.1752941
15. Zhang JJ. Adaptive multi-dimensional Taylor network dynamic surface control for a class of strict-feedback uncertain nonlinear systems with unmodeled dynamics and output constraint. *ISA Trans*. 2021;108:35-47. doi:10.1016/j.isatra.2020.08.035
16. Han YQ. Adaptive tracking control for a class of stochastic non-linear systems with input delay: a novel approach based on multi-dimensional Taylor network. *IET Control Theory Appl*. 2020;14(15):2147-2153. doi:10.1049/iet-cta.2020.0336
17. Wang MX, Zhu SL, Liu SM, Du Y, Han YQ. Design of adaptive finite-time fault-tolerant controller for stochastic nonlinear systems with multiple faults. *IEEE Trans Automat Sci Eng*. 2022;1-11. doi:10.1109/TASE.2022.3206328
18. Zhang C, Yan HS. Multidimensional Taylor network adaptive control for MIMO time-varying uncertain nonlinear systems with noises. *Int J Robust Nonlinear Control*. 2020;30(1):397-420. doi:10.1002/rnc.4774
19. Chu L, Gao T, Wang MX, Han YQ, Zhu SL. Adaptive decentralized control for large-scale nonlinear systems with finite-time output constraints by multi-dimensional Taylor network. *Asian J Control*. 2022;24(4):1769-1779. doi:10.1002/asjc.2571
20. Yan HS, Han YQ. Decentralized adaptive multi-dimensional Taylor network tracking control for a class of large-scale stochastic nonlinear systems. *Int J Adapt Control Signal Proces*. 2019;33(4):664-683. doi:10.1002/acs.2978
21. Chen M, Zhou YL, Guo WW. Robust tracking control for uncertain MIMO nonlinear systems with input saturation using RWNNDO. *Neurocomputing*. 2014;144:436-447. doi:10.1016/j.neucom.2014.04.032
22. Li HY, Bai L, Zhou Q, Lu RQ, Wang LJ. Adaptive fuzzy control of stochastic nonstrict-feedback nonlinear systems with input saturation. *IEEE Trans Syst Man Cybern Syst*. 2017;47(8):2185-2197. doi:10.1109/TSMC.2016.2635678
23. Gao YF, Sun XM, Wen CY, Wang W. Adaptive tracking control for a class of stochastic uncertain nonlinear systems with input saturation. *IEEE Trans Automat Control*. 2017;62(5):2498-2504. doi:10.1109/TAC.2016.2600340
24. Ming HF, Xu SY, Zhang BY, Ma Q. Output-feedback control for stochastic nonlinear systems subject to input saturation and time-varying delay. *IEEE Trans Automat Control*. 2019;64(1):359-364. doi:10.1109/TAC.2018.2828084
25. Zhou Q, Shi P, Tian Y, Wang MY. Approximation-based adaptive tracking control for MIMO nonlinear systems with input saturation. *IEEE Trans Cybern*. 2015;45(10):2119-2128. doi:10.1109/TCYB.2014.2365778
26. Liu L, Gao TT, Liu YJ, Tong SC. Time-varying asymmetrical BLFs based adaptive finite-time neural control of nonlinear systems with full state constraints. *IEEE/CAA J Automat Sin*. 2020;7(5):1335-1343. doi:10.1109/JAS.2020.1003213
27. Li HY, Zhao SY, He W, Lu RQ. Adaptive finite-time tracking control of full state constrained nonlinear systems with dead-zone. *Automatica*. 2019;100:99-107. doi:10.1016/j.automatica.2018.10.030
28. Wang YD, Zong GD, Yang D, Shi KB. Finite-time adaptive tracking control for a class of nonstrict feedback nonlinear systems with full state constraints. *Int J Robust Nonlinear Control*. 2022;32(5):2551-2569. doi:10.1002/rnc.5777
29. Li N, Han YQ, He WJ, Zhu SL. Control design for stochastic nonlinear systems with full-state constraints and input delay: a new adaptive approximation method. *Int J Control Automat Syst*. 2022;20(8):2768-2778. doi:10.1007/s12555-021-0451-z
30. Han YQ. Adaptive control of a class of stochastic nonlinear systems with full state constraints and input saturation using multi-dimensional Taylor network. *Asian J Control*. 2022;24(4):1609-1621. doi:10.1002/asjc.2551
31. Gao TT, Liu YJ, Li DP, Tong SC, Li TS. Adaptive neural control using tangent time-varying BLFs for a class of uncertain stochastic nonlinear systems with full state constraints. *IEEE Trans Cybern*. 2021;51(4):1943-1953. doi:10.1109/TCYB.2019.2906118
32. Wei Y, Zhou PF, Wang YY, Duan DP, Zhou WX. Adaptive neural dynamic surface control of MIMO uncertain nonlinear systems with time-varying full state constraints and disturbances. *Neurocomputing*. 2019;364:16-31. doi:10.1016/j.neucom.2019.07.033
33. Zhao K, Song YD, Zhang ZR. Tracking control of MIMO nonlinear systems under full state constraints: a single-parameter adaptation approach free from feasibility conditions. *Automatica*. 2019;107:52-60. doi:10.1016/j.automatica.2019.05.032
34. Zhang Q, Zhai D, Dong JX. Observer-based adaptive fuzzy decentralized control of uncertain large-scale nonlinear systems with full state constraints. *Int J Fuzzy Syst*. 2019;21(4):1085-1103. doi:10.1007/s40815-018-0595-z
35. Zhang J, Li S, Ahn CK, Xiang ZR. Adaptive fuzzy decentralized dynamic surface control for switched large-scale nonlinear systems with full-state constraints. *IEEE Trans Cybern*. 2022;52(10):10761-10772. doi:10.1109/TCYB.2021.3069461
36. Zhou SY, Song YD. Prescribed performance neuroadaptive fault-tolerant compensation for MIMO nonlinear systems under extreme actuator failures. *IEEE Trans Syst Man Cybern Syst*. 2021;51(9):5427-5436. doi:10.1109/TSMC.2019.2954875

37. Wang HQ, Bai W, Zhao XD, Liu PXP. Finite-time-prescribed performance-based adaptive fuzzy control for strict-feedback nonlinear systems with dynamic uncertainty and actuator faults. *IEEE Trans Cybern*. 2022;52(7):6959-6971. doi:10.1109/TCYB.2020.3046316
38. Wang HQ, Zou YC, Liu PXP, Liu XP. Robust fuzzy adaptive funnel control of nonlinear systems with dynamic uncertainties. *Neurocomputing*. 2018;314:299-309. doi:10.1016/j.neucom.2018.06.053
39. Han YQ, Li N, He WJ, Zhu SL. Adaptive multi-dimensional Taylor network funnel control of a class of nonlinear systems with asymmetric input saturation. *Int J Adapt Control Signal Proces*. 2021;35(5):713-726. doi:10.1002/acs.3224
40. Zong GD, Wang YD, Karimi HR, Shi KB. Observer-based adaptive neural tracking control for a class of nonlinear systems with prescribed performance and input dead-zone constraints. *Neural Netw*. 2022;147:126-135. doi:10.1016/j.neunet.2021.12.019
41. Shao XF, Tong SC. Adaptive fuzzy prescribed performance control for MIMO stochastic nonlinear systems. *IEEE Access*. 2018;6:76754-76767. doi:10.1109/ACCESS.2018.2882634
42. Zhu SL, Han YQ. Adaptive decentralized prescribed performance control for a class of large-scale nonlinear systems subject to nonsymmetric input saturations. *Neural Comput Applic*. 2022;34:11123-11140. doi:10.1007/s00521-022-07032-8
43. Han YQ. Design of decentralized adaptive control approach for large-scale nonlinear systems subjected to input delays under prescribed performance. *Nonlinear Dyn*. 2021;106:565-582. doi:10.1007/s11071-021-06843-z
44. Li YM, Tong SC. Prescribed performance adaptive fuzzy output-feedback dynamic surface control for nonlinear large-scale systems with time delay. *Inform Sci*. 2015;292:125-142. doi:10.1016/j.ins.2014.08.060
45. Han YQ, He WJ, Li N, Zhu SL. Tracking control for large-scale switched nonlinear systems subject to asymmetric input saturation and output hysteresis: a new adaptive network-based approach. *Int J Robust Nonlinear Control*. 2022;32(14):8052-8072. doi:10.1002/rnc.6258
46. Si WJ, Dong XD. Adaptive neural control for MIMO stochastic nonlinear pure-feedback systems with input saturation and full-state constraints. *Neurocomputing*. 2018;275:298-307. doi:10.1016/j.neucom.2017.08.038
47. Min HF, Xu SY, Zhang ZQ. Adaptive finite-time stabilization of stochastic nonlinear systems subject to full-state constraints and input saturation. *IEEE Trans Automat Control*. 2021;66(3):1306-1313. doi:10.1109/TAC.2020.2990173
48. Li YL, Niu B, Zong GD, Zhao JF, Zhao XD. Command filter-based adaptive neural finite-time control for stochastic nonlinear systems with time-varying full-state constraints and asymmetric input saturation. *Intl J Syst Sci*. 2022;53(1):199-221. doi:10.1080/00207721.2021.1943562
49. Han YQ, Yan HS. Adaptive multi-dimensional Taylor network tracking control for SISO uncertain stochastic non-linear systems. *IET Control Theory Appl*. 2018;12(8):1107-1115. doi:10.1049/iet-cta.2017.0538

How to cite this article: Li N, Du Y, Wang D-M, Zhu S-L, Han Y-Q. Adaptive decentralized prescribed performance control for a class of large-scale stochastic nonlinear systems subject to input saturation and full state constraints. *Int J Adapt Control Signal Process*. 2023;37(9):2451-2471. doi: 10.1002/acs.3647